Gondwana Research 110 (2022) 143–164

Contents lists available at ScienceDirect

Gondwana Research

journal homepage: www.elsevier.com/locate/gr

GR Focus Review

The Columbia supercontinent: Retrospective, status, and a statistical assessment of paleomagnetic poles used in reconstructions

Joseph G. Meert [a,*], M. Santosh [b,c]

[a] Department of Earth & Planetary Sciences, University of Florida, Gainesville, FL 32611, USA
[b] School of Earth Sciences and Resources, China University of Geosciences, Beijing 100083, China
[c] Department of Earth Science, University of Adelaide, Adelaide, SA 5005, Australia

ARTICLE INFO

Article history:
Received 12 June 2022
Revised 25 June 2022
Accepted 27 June 2022
Available online 30 June 2022
Handling Editor. S. Kwon

Keywords:
Columbia
Paleomagnetism
SAMBA
Reconstructions
Bayesian statistics

ABSTRACT

The proposal that a Paleo-Mesoproterozoic supercontinent, Columbia, preceded the existence of Rodinia was forwarded in 2002. A similar proposal that same year provided a detailed discussion of 2.1–1.8 Ga orogenic belts distributed throughout the globe thought to represent the assembly of Columbia. In the 20 years that followed, evidence in favor of Columbia has grown but its exact configuration and geometrical relationships between various cratons remains elusive. One of several challenges in reconstructing Columbia is the paucity of high-quality paleomagnetic data. Progress is slow, but steady, in this realm as it requires painstaking field and laboratory work to generate a new pole. Despite large gaps in the database, we have generated testable models of Columbia. Unfortunately, there are seldom coeval poles from many continents and reconstructions represent small time-slices in Columbia's lifespan. In this contribution, we review the history of the Columbia hypothesis, evidence mounted in support of the idea and status of the model. We present a statistical method to evaluate goodness of fit in paleomagnetically based reconstructions where data are separated in both time and space. Baltica and Amazonia are often linked together with eastern Laurentia to form a long-lived accretionary orogenic margin of Columbia. This so-called SAMBA model was originally posited as a one billion year long (1.8–0.8 Ga) fixture in both Columbia and Rodinia. Paleomagnetic data are supportive of this connection from ~ 1.75–1.5 Ga, but not during younger times. We also test a recent model of Columbia based on the highest quality paleomagnetic poles available at that time. Our analysis reveals numerous discrepancies between data and models that will need to be addressed as work towards reconstructing Columbia continues unabated.

Contents

* Corresponding author.
E-mail address: jmeert@ufl.edu (J.G. Meert).

https://doi.org/10.1016/j.gr.2022.06.014
1342-937X/

1. Introduction

Professor John James William Rogers (J.J.W. Rogers, Fig. 1) who passed away on 14 January 2015 at the age of 84, was one of the doyens in the field of geology. His research interests covered a wide range of topics including sedimentology, igneous petrology, geochemistry and isotope geochronology, environmental geology, and geoarchaeology, among other themes, and his contributions were published as research papers in various journals as well as in authored and edited books. After John moved to the University of North Carolina at Chapel Hill in 1975, he was actively involved in several international collaborations including with researchers in India, Saudi Arabia, Egypt, Libya, Puerto Rico, Tunisia, Mexico, and Costa Rica, and he started focusing his interest on the evolution of continents and supercontinents. In 1993, he proposed the Earth's oldest supercontinent Ur which was assembled at 3.0 Ga (Rogers, 1993), and subsequently brought out an outstanding summary on the configuration of the various supercontinents in earth history (Rogers, 1996). Thereafter, he contacted M. Santosh who was at that time leading a major international project on the Gondwana supercontinent, which marked the beginning of a long collaboration and friendship until John passed away. John shared his innovative ideas with Santosh on a Paleo-Mesoproterozoic supercontinent that attained maximum close packing and incorporated majority of the continental fragments on the globe at that time. Their collaboration eventually led to the proposal of the globe's first coherent supercontinent which was named as "Columbia", with a landmark publication on the configuration of this Paleo-Mesoproterozoic supercontinent in Gondwana Research (Rogers and Santosh, 2002) that attracted wide global attention including that of the media. This paper stands as the highest cited article in GR and enthused several studies from various parts of the world in understanding the history, evolution, and disruption of this supercontinent. They co-authored the book "Continents and Supercontinents" (Rogers and Santosh, 2004), which is now a valuable reference for teaching. Despite his long illness, frequent hospital visits, and difficulties with daily life, John continued his interest in science, including publishing an updated work on the tectonic and surface effects of the Columbia supercontinent (Rogers and Santosh, 2009). In a special issue of GR published in his honor in 2003, John wrote an autobiographic sketch (Rogers, 2003), which stands as testimony to his glorious life and career. Referring to his milestone paper Rogers (1996), John shared his experience: "I wrote a general paper on the three old continents and …. the paper was rejected three times, twice with regret and once with contempt, before it was published in the Journal of Geology in 1996". He also wrote that: "I have always regarded plate tectonics as a codification of ideas rather than an independent process, its importance being that this codification gave geologists an enhanced opportunity to look at their individual work and wonder more clearly what their studies contributed to understanding the general history of the earth".

This year (2022) marks the 20th anniversary of the proposal of Columbia and the publication of the Rogers and Santosh (2002) paper in GR, when we remember John's glorious life and career, his knowledgeable contributions to geoscience, and his insightful proposals on the history of the formation and evolution of supercontinents which enhanced our understanding of Earth history, geodynamics, and the evolution of life and environment on our planet.

Fig. 1. John J.W. Rogers Professor of Geology North Carolina (b. 6/27/1930 d. 1/14/2015). John received his B.S. degree in 1952 from CalTech and his Ph.D. in 1955 from the same institution. He originated the idea of the Columbia supercontinent in 2002.

1.1. The original Columbia supercontinent

Rogers (1996) proposed that three large cratonic nuclei which stabilized by at least 2.0 Ga were integral parts of all younger supercontinents. At that time, only two supercontinents had been proposed (Rodinia and Pangea). Rogers named these three 'stable' blocks Atlantica (2.0 Ga stabilization; Fig. 2a), Arctica (2.5 Ga stabilization; Fig. 2b) and Ur (3.0 Ga stabilization; Fig. 2c) and argued that their disaggregation did not occur until the breakup of Rodinia (Arctica) and Pangea (Atlantica and Ur). This hypothesis required that the several of the orogenic belts found throughout Gondwana (Brasiliano, Damara, Malagasy, Kuunga) were intracratonic (or internal with limited separation) which he admitted was a highly controversial idea. Subsequent work shows that most of these belts formed during the Neoproterozoic-Cambrian assembly of Gondwana following the breakup of the Rodinia supercontinent and were intercratonic in origin (Meert et al., 1995; Stern, 1994; Meert, 2003; Collins and Pisarevsky, 2005; Gray et al., 2008; Meert and Lieberman, 2008). Similarly, the Proterozoic orogenic belts found throughout Arctica are now thought to be intercratonic (see Zhao et al., 2002 for example). Although the concept of these three long-lived nuclei is now less tenable, Meert (2014) also noted that many of the components within Rogers (1996) core elements seemed to behave as 'strange attractors' positioned in more, or less, the same configuration within the Columbia, Rodinia and Pangea supercontinents.

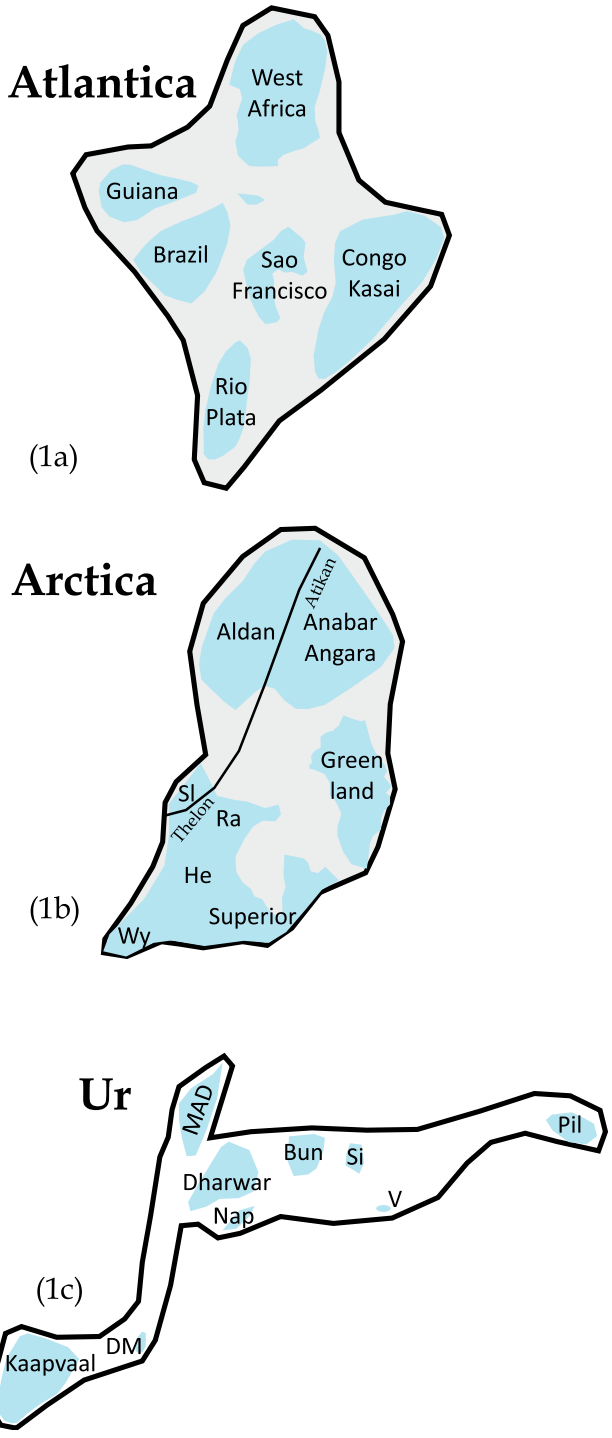

Fig. 2. The building blocks of the Columbia supercontinent according to Rogers, 1996; (a) Atlantica comprised of the cratonic elements of South America and western and central Africa; (b) Arctica comprised of Siberia, Greenland and cratonic North America; (c) Ur comprised of South Africa, Madagascar, E. Antarctic cratons, India and western Australia.

In 2002, Rogers and Santosh proposed that a supercontinent (Columbia) existed sometime between 1.9 and 1.5 Ga and disaggregated around 1.4 Ga (Rogers and Santosh, 2002). The original configuration for this supercontinent was based on correlations between the Mahanadi, Prahnita-Godavari, Kurduvadi and Kayana Rift basins in India with the Belt-Purcell, Uinta, Unkar and Apache sequences in western Laurentia (Fig. 3a; the Columbia River region of North America). Columbia included the ancient cores of Ur, Atlantica and Arctica and Paleoproterozoic additions to those regions (Fig. 3b) and positioned East Gondwana along the present-day western margin of Laurentia with Siberia and Baltica along the Arctic and Greenland margins of Laurentia respectively. Columbia also featured the Zimbabwe and Kalahari cratons as part of East Gondwana near the SW corner of Laurentia (expanded "Ur"). NW Africa and South America were separated from the East Gondwana landmass by a narrow Chewore Ocean (Fig. 3b). The main evidence marshalled in support of their configuration were the ages of rifting and widespread ~ 1.9–1.8 Ga collisional orogens. As is the case with many important discoveries, Rogers and Santosh were not alone in making these observations. Zhao et al. (2002) wrote a paper working its way through the editorial review process wherein they referred to the Paleoproterozoic supercontinent as "Hudson" which was changed to "Columbia" during final editing due to the Rogers and Santosh (2002) paper already in print.

Meert (2012) reviewed the history of the Columbia supercontinent and the controversy over whether "Columbia" or "Nuna" (Hoffman, 1997) held precedence. Meert (2012) argued that while the term Nuna appeared before Columbia, Nuna was composed only of Siberia, Laurentia and Baltica and should properly be viewed as the core of "Nena" (Gower et al., 1990; Rogers, 1996). The controversy over the name continues unabated; however recent publications (Mitchell et al., 2021; Wang et al., 2021a) offered the same 'novel' solution for dubbing the supercontinent Columbia as did Meert (2012) . . .namely that Nuna was an integral part of the larger Columbia supercontinent.

Meert (2002) evaluated the paleomagnetic evidence at the for the Columbia model of Rogers and Santosh (2002). That study concluded that any supercontinent must be younger than ~ 1.8 Ga based upon limited paleomagnetic data. Meert (2002) was unable to demonstrate the proposed links between southern India and western Laurentia due to a near-complete lack of data from India. Subsequent paleomagnetic, geological and geochronological data demonstrated that many of the core elements of Columbia were not fully assembled until ~ 1.8–1.7 Ga (Bogdanova et al., 2008; Payne et al., 2009; Killian et al., 2016; Meert and Santosh, 2017; Meert et al., 2021; Kirscher et al, 2021a). Meert and Santosh (2017) provided an overview of the Columbia hypothesis.

2. Columbia in 2022: State of the science

There are several key observations that were used to support the idea of a Paleo-Mesoproterozoic supercontinent that remain valid. Chief amongst them is the ubiquitous presence of 2.1–1.8 Ga orogenic belts noted by Rogers and Santosh (2002) and in the detailed publication of Zhao et al. (2002). Zhao et al. (2002) also noted widespread 'anorogenic magmatism' during the 1.4–1.2 Ga interval is thought to reflect the initial breakup of Columbia.

There is some consensus that Columbia existed in some configuration during the interval from ~ 1750 Ma until its 'breakup' around 1.3–1.4 Ga; however, the exact configuration and lifespan remains elusive. Meert (2014) pointed out the obvious similarities between Rodinia and Columbia and argued that this may reflect an underlying bias in perception (Laurentia-centric) or that plate tectonics operated in a different fashion (see also Stern, 2018). There have been numerous attempts to model Columbia since Zhao et al. (2002) created a reconstruction based on the geometric/age relationships of orogenic belts within Columbia. We see the following as key questions that are unresolved at the present time and therefore require additional work before a reasonable approximation of Columbia can be achieved.

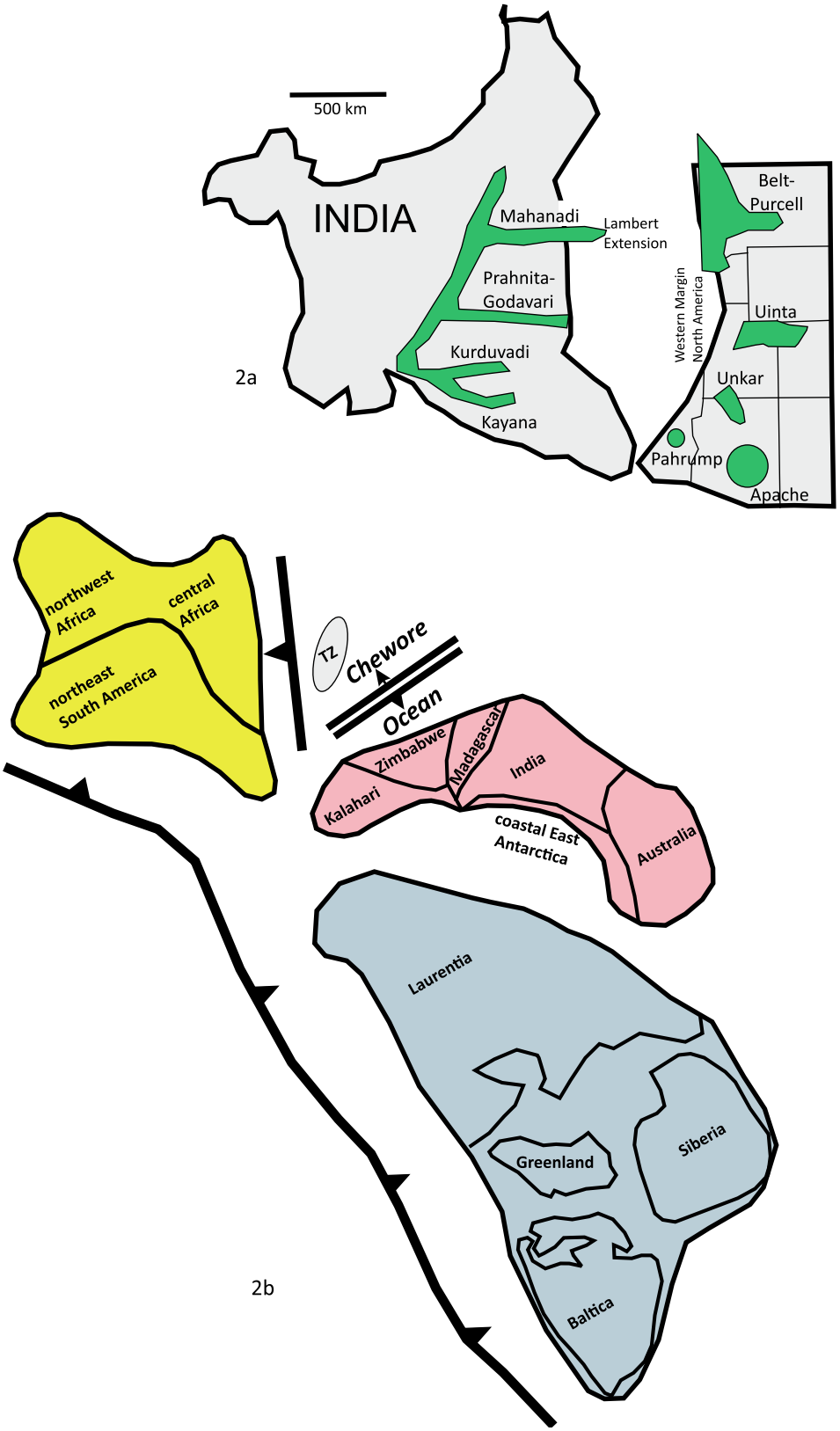

Fig. 3. (a) Rogers and Santosh (2002) proposed fit between the ~ 1450 Ma rift basins in India and western North America supporting the (b) "Columbia" supercontinental reconstruction.

(1) Zhao et al. (2002) outlined the available geochronological data for many of the Paleoproterozoic orogenic belts around the globe. The ages for some of these belts (particularly around the core Nuna blocks) are well-constrained and geological correlations seem well founded. Elsewhere, collisional ages are poorly constrained or incorrect (see Meert

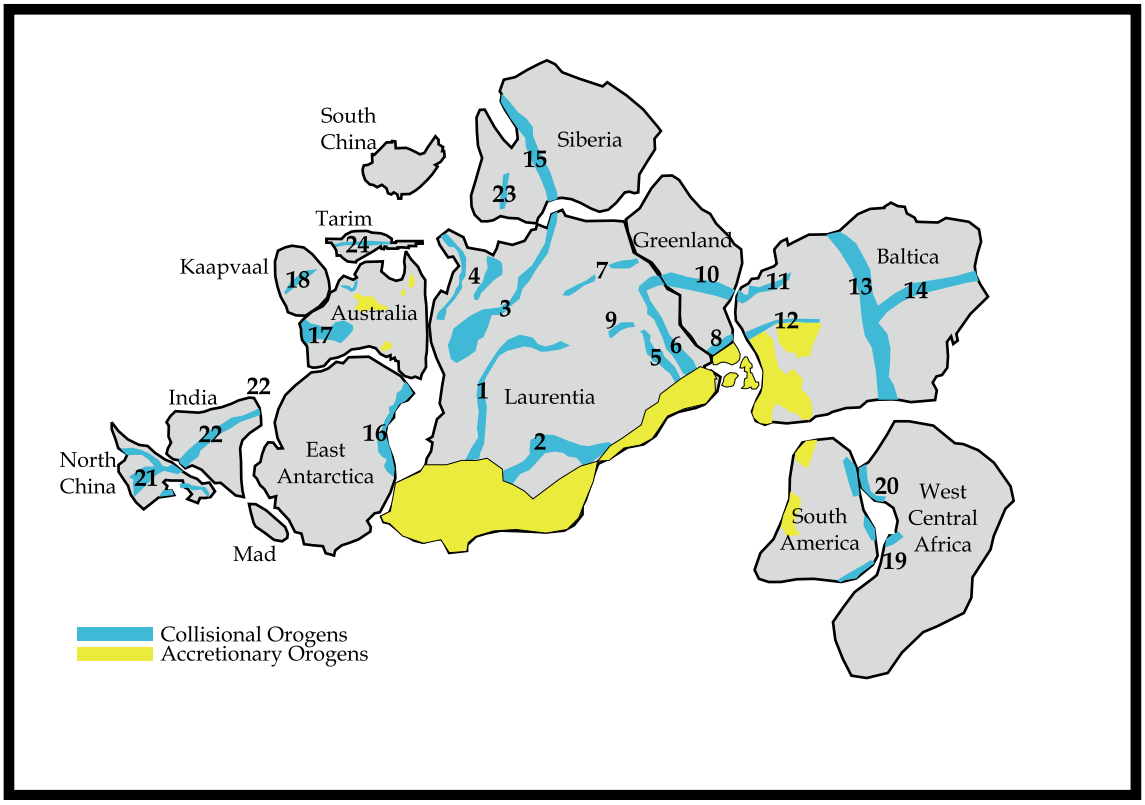

Fig. 4. Orogenic belts thought to have developed during the assembly of the Columbia supercontinent according to Zhao et al. (2002) and Wu et al. (2020). 1. Trans-Hudson; 2. Penokean; 3. Taltson-Thelon; 4. Wopmay; 5. New Quebec; 6. Torngat; 7. Foxe; 8. Makkovik-Ketlidian; 9. Ungava; 10. Nagsugtoqidian; 11. Kola-Karelian; 12. Svecofennian; 13. Volhyn-Central Russian; 14. Pachelma; 15. Akitkan; 16. Transantarctic; 17. Capricorn; 18. Limpopo; 19. Transmazonian; 20. Eburnean; 21. Trans-North China; 22. Central Indian Tectonic Zone; 23. Central Aldan; 24. Central Tarim.

et al., 2021; Wang et al., 2021b for example). Many of the orogenic belts link smaller nuclei within a single larger continent but it is more difficult to correlate the belts on a global scale.

(2) Limited paleomagnetic data for many regions. The paleomagnetic database has expanded since the initial Columbia proposal (see Evans et al., 2021) but significant (>100 Ma) gaps exist in the current database for many individual blocks comprising the supercontinent.

(3) It is now recognized that interior cratonic regions of Australia and Siberia underwent relative rotation (see Zhang et al., 2012; Evans et al., 2016) which must be accounted for when making paleogeographic reconstructions. More recently, there are proposals of intracratonic rotations within the Dharwar craton of India and between the Singhbhum and Dharwar cratons (see Pivarunas and Meert, 2020; Pivarunas et al., 2021) for complete discussion). Small rotations within individual cratons can result in misfits between similar-age poles. Unfortunately, a robust analysis of proposed rotations requires one or more coeval poles from each of the rotated blocks and a reasonable geological explanation for those rotations.

(4) Geochronological and isotopic data might provide important clues about the timing of supercontinent assembly and dispersal (Condie and Aster, 2010; Hawkesworth et al., 2013) but not necessarily about the geometry of the supercontinent. There is some controversy about how well the detrital zircon record aligns with supercontinent assembly and dispersal; however, the zircon record is more robust than our knowledge of the geometry of Columbia (Condie et al., 2017). Recent data indicate that Columbia may not have fully formed until ~ 1.6 Ga (Kirscher et al., 2021b; Volante et al., 2022) which considerably shortens the lifespan of the Columbia supercontinent.

2.1. Orogenies and orogenic belts

While the original proposal for Columbia by Rogers and Santosh (2002) was based on correlations between rift basins in India and Laurentia, they acknowledged that evidence for the collisional orogenesis that brought them together was enigmatic. Zhao et al. (2002) used orogenic belts of purported 2.1–1.8 Ga age as the foundation of their proposal (Fig. 4). In attempting to piece together the geometry of Columbia, orogenic belts are the common focal point of reconstructions (Zhao et al., 2003; Johansson, 2009; Reis et al., 2013; Pehrsson et al., 2015; Terentiev and Santosh, 2020; Wan et al., 2020).

Orogens are broadly classified as accretionary or collisional (Cawood et al., 2009). Accretionary orogens, or peripheral orogens, typically form along the boundary between oceanic and continental plates and are the locus of subduction, terrane accumulation and juvenile crust formation (constructive). The Central Asian Orogenic Belt (CAOB) is the best example of an accretionary orogen in the Phanerozoic. Collisional orogens mark the boundaries between two (or more) formerly distinct continental blocks. They are usually located in the interior regions of an assembled continent (or supercontinent). Collisional orogens may form the site of new oceanic crust formation during subsequent continental breakup. Phanerozoic examples of accretionary orogens include the Andean-Cordilleran margins of South-Central-North America and the Central Asian Orogenic Belt. Collisional orogenic belts associated with the assembly of Gondwana include the Brasiliano,

Table 1
List of Orogens Associated with Columbia Assembly.

Orogen	Type	Crustal Elements	Age Range (Ga)	Reference
N. America				
Trans-Hudson	Collisional	Superior-Churchill	1.92–1.795	Darbyshire et al., 2017; Zhao et al., 2002; Chiarenzelli et al., 1998
Penokean	Accretional	Superior-Marshfield	1.89–1.83	Zi et al., 2021
Taltson-Thelon	Collisional/ Accretional	Slave-Rae-Hearne	2.01–1.97	Davis et al., 2021
Wopmay	Accretional	Slave-Hottah	1.9–1.875	Hildebrand et al., 2010
New Quebec	Collisional/ Accretional	Superior-Core zone microcontinents	1.87–1.77	Godet et al., 2020
Torngat	Collisional	Core Zone MC-North Atlantic craton	1.89–1.81	Charette et al., 2021
Foxe	Accretional	Rae-THO	1.87–1.85	Whitmeyer and Karlstrom, 2007
Great Falls TZ	Collisional	Wyoming- Medicine Hat	1.85–1.80	Whitmeyer and Karlstrom, 2007
Ungava	Collisional	Rae-Narsajuq-NE Superior craton	1.86–1.82	Whitmeyer and Karlstrom, 2007
Makkovik-Ketilidian	Accretional	Keipokuk/Adlavik arcs-N. Atlantic craton	1.93–1.64	Hinchey, 2021; Zhao et al., 2002; Johansson et al., 2022
Naggsugtuqidian	Collisional	N. Atlantic-Rae-Ammassalik	1.88–1.84	Kolb, 2014; Zhao et al., 2002
Yavapai	Accretionary	Various arcs/fragments	1.8–1.7	Johansson et al., 2022
Mazatzal	Accretionary	Various arcs/fragments	1.65–1.60	Johansson et al., 2022
Fennoscandia				
Kola-Karelia	Collisional	Karelia-Kola cratons	2.3–1.90	Zhao et al., 2002
Svecofennian	Accretional	Arcs and Karelian craton	2.0–1.75	Zhao et al., 2002
Volhyn-Central Russian	Collisional	Volgo-Uralia-Sarmatia-Fennoscandia	1.9–1.8	Condie, 2013; Bogdanova, 1999
Volga-Don	Collisional	Volgo-Uralia-Sarmatia	2.1–1.9	Bogdanova, 1999; Johansson et al., 2022
Siberia				
Angara	Accretional/ Collisional		1.9–1.8	Donskaya, 2020
Akitkan	Collisional	Anabar-Aldan cratons	2.06–1.9	Donskaya, 2020
Cis-Stanavoy	Collisional	Stanavoy-Aldan	1.95–1.9	Donskaya, 2020
Hapschan	Collisional	Birekte-Anabar	2.0–1.95	Donskaya, 2020
Tirkand	Collisional	East Aldan-West Aldan	1.95–1.9	Donskaya, 2020
South America (SAM)				
Trans-Amazonian	Collision	Guiana-Guapore Shields	2.26–1.93	Neves, 2021
Ventauri-Tapajos	Accretionary	Juvenile crust	2.01–1.80	Vasquez et al., 2019
Rio Negro-Juruena	Accretionary	Juvenile crust	1.82–1.60	Cordani et al., 2016
Rondonian-San Ignacio	Accretionary	Juvenile crust	1.59–1.30	Texeira et al., 2020
West Africa				
Birimian-Eburnian	Accretionary	Arc terranes, W. Africa-SAM	2.27–1.96	Grenholm, 2019;
Central Africa-SAM				
Eburnian	Collisional	Congo-Sao Francisco-SAM	2.2–1.98	Weber et al., 2016.
North China				
Trans North China Orogen	Collisional	Western Block and Eastern Block	1.92–1.82	Liu et al., 2020
India				
Central Indian Tectonic Zone	Accretionary	Arc terranes	1.65–1.55	Bhowmik, 2019
Australia				
Capricorn	Collisional	Yilgarn-Pilbara	2.21–1.95	Cawood and Tyler, 2004; Johnson et al., 2013
Congo-Sao Francisco				
Ubendian-Usagaran-Ruzizian	Accretionary/ Collisional	Bangwelu-Tanzanian craton and arc terranes	2.1–1.8	Boniface and Tsujimori, 2021
Tarim				
Central Tarim	Collisional	North-South Tarim cratons	1.96–1.90	Wu et al., 2020; Wang et al., 2020
Peripheral Tarim	Accretionary/ Collisional	Tarim and??	1.86–1.80	Wu et al., 2020

Damara, East Africa, Kuunga and Pinjarra (Stern, 1994; Collins, 2003; Gray et al., 2008; Meert and Lieberman, 2008; Markwitz et al., 2017). Pangea assembly resulted in the Variscan-Caledonide-Appalachian orogenic belts. The breakup of Pangea exploited these and older collisional orogens during the opening of the Atlantic (Brasliano-Appalachian-Variscan-Caledonian), Indian (East Africa, Kuunga, Eastern Ghats) and Southern (East Africa, Kuunga, Pinjarra, Kimban-Strangways) oceans during the Mesozoic.

The formation of Rodinia is associated with "Grenville-age' (~1100–900 Ma) collisional orogens. These include the Grenville (Laurentia), Sveconorwegian (Baltica), Eastern Ghats (India), Namaqua (Kalahari), Sunsas (Amazonia).

Many of the orogenic belts that formed during the Paleoproterozoic-Mesoproterozoic assembly of Columbia are classified as accretional (Table 1; modified from Perhsson et al., 2015). Condie (2013) refers to the "great Proterozoic accretionary orogen" that formed along the margins of Laurentia, Baltica and Amazonia (Fig. 5). The model posits a long-lived accretionary margin beginning in the Paleoproterozoic and continuing into the Mesoproterozoic with progressive outboard growth of juvenile terranes. Recent discoveries of orogenic belts associates with

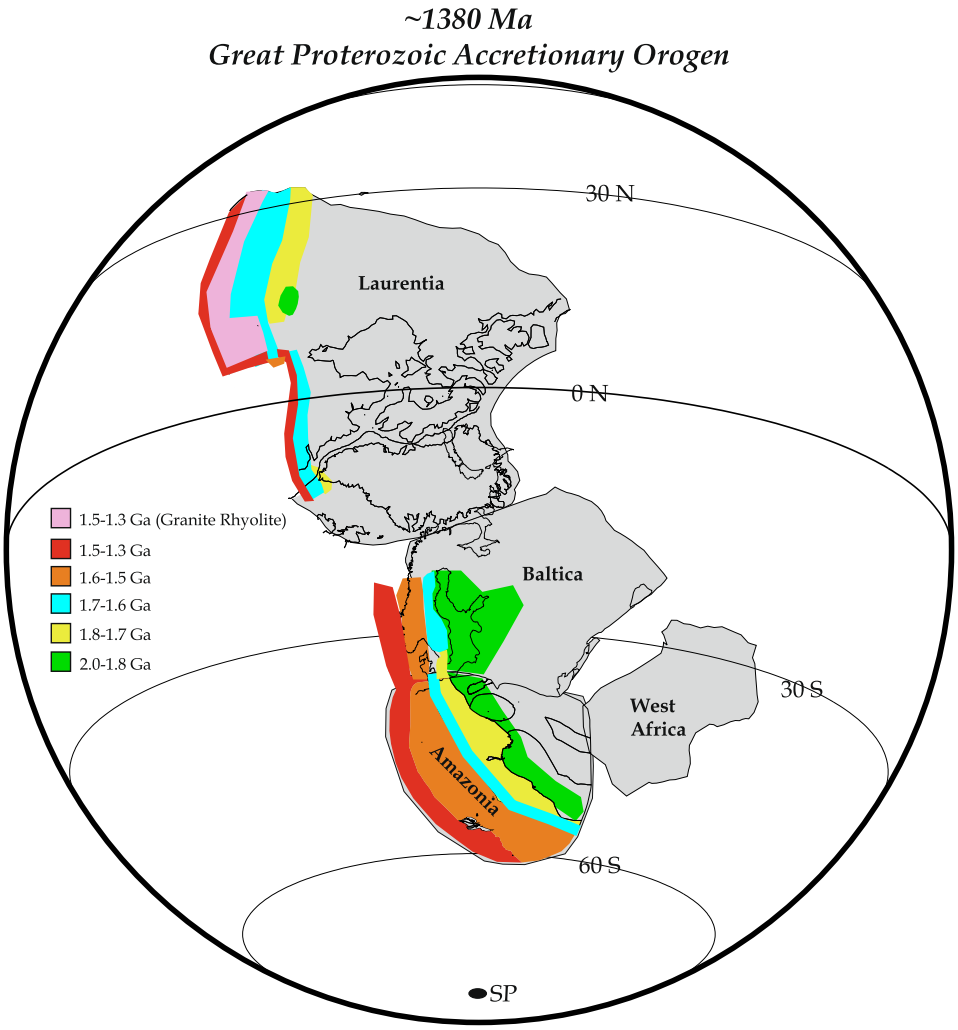

Fig. 5. "Great Accretionary Orogeny" that was hypothesized along the margins of Eastern Laurentia, Baltica and Amazonia during the lifespan of the Columbia supercontinent. The relationship between Amazonia and Baltica is equivalent to the SAMBA hypothesis of Johannson (2009) and the larger connection according to Johannson et al. (2022).

Columbia assembly were documented in the Tarim craton (Wu et al., 2020; Wang et al., 2020).

2.2. Paleomagnetic based reconstructions

Paleomagnetic studies begin with the fundamental assumption that the Earth's magnetic field closely approximates a Geocentric axial dipole (GAD; Meert, 2009). Although significant departures from GAD were proposed for the Precambrian (Kent and Smethurst, 1998; Piper and Grant, 1989; Williams and Schmidt, 2004), others (Evans, 2006; Swanson-Hysell et al., 2009; Panzik and Evans, 2014) argue that GAD is a reasonable assumption for most of the Proterozoic. Veikkolainen and Pesonen (2021) make a case for a ~ 23% octupolar component from 1200 to 1900 Ma; however, the paleomagnetic database is quite limited and may simply reflect a low-latitude position for many of the cratonic elements during that interval (Meert et al., 2003). The major exception may occur in the Ediacaran interval from ~ 600–550 Ma where the geomagnetic field intensity is ultra-low and disparate paleomagnetic directions are present in coeval rocks (Abrajevitch and Van der Voo, 2010; Bono et al., 2019; Thallner et al., 2021a, b; Thallner et al., 2022). Recently, Sears (2022) argued for a significant quadrupolar contribution during the Paleoproterozoic-Meso proterozoic interval; however, that study evaluated paleomagnetic data from Laurentia and Siberia rather than a global analysis. In the following discussion, we proceed with the assumption that the GAD hypothesis most closely approximates the Earth's magnetic field in the Proterozoic.

A single paleomagnetic pole can be used to place the continent in either the northern or southern hemisphere and at any longitude due to the symmetry of the geomagnetic field (Meert, 2009). The 'closest approach' technique (Meert and Torsvik, 2003) uses these degrees of freedom to provide the optimal fit between two continents. We provide an example using India-Laurentia at two distinct time periods which provide a test of the original Rogers and Santosh (2002) India-Laurentia fit. Our reconstruction at ~ 1750 Ma (Fig. 6a) is based on the Laurentian Cleaver dykes pole (1740 +/- 5 Ma; Irving et al., 2004) and a 1765 Ma pole from the Singhbhum craton (Shankar et al., 2017; Pivarunas et al., 2021). A mean Laurentian paleomagnetic pole from six different studies with ages ~ 1460 Ma (Swanson-Hysell, 2021) yields a result at 13.3° S, 215.7° N (A95 = 12°). Pisarevsky et al. (2013) studied a sequence of similar-age dykes (1466 Ma) in the Bastar craton of India which yielded a mean paleomagnetic pole at 35.7° N, 132° E (A95 = 15.5°). Fig. 6b shows a reconstruction based on these two ~ 1460 Ma poles. In both cases, the "Columbia" fit proposed by Rogers and Santosh (2002, 2009) is not compatible with the extant paleomagnetic data. The closest approach technique does

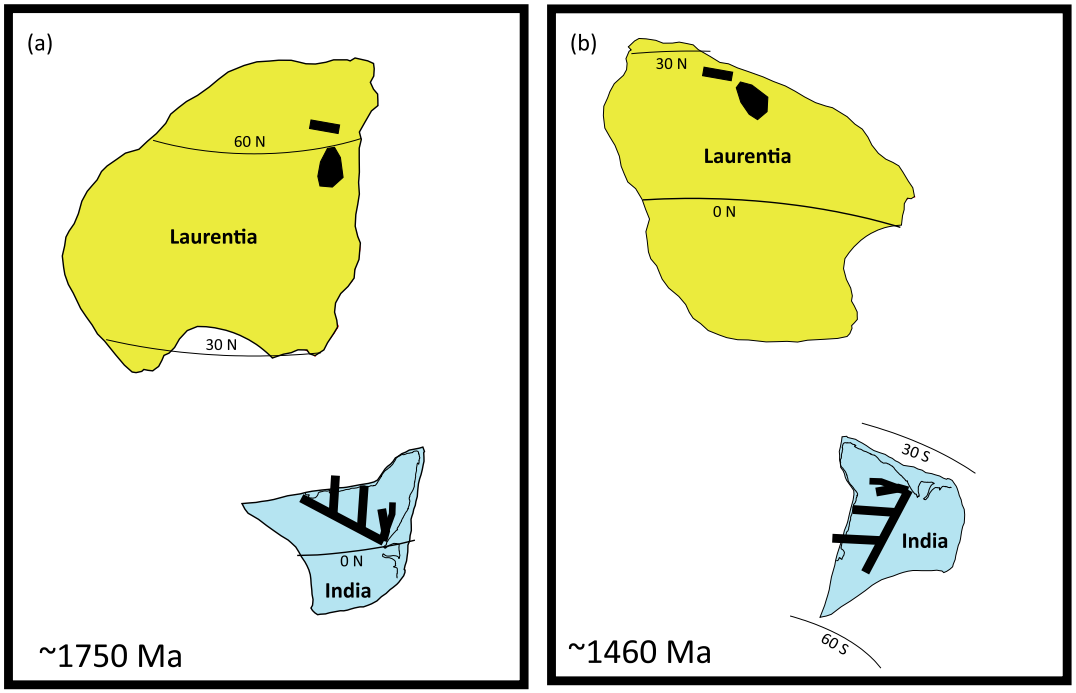

Fig. 6. A test of the "Columbia" fit between western Laurentia and India at (a) ~ 1750 Ma and (b) 1460 Ma demonstrating the latitudinal differences between the two cratons at those times. It is possible to choose the alternative polarity at 1460 Ma which will position India in a more favorable latitudinal location, but the basin fits proposed by Rogers and Santosh (2002) will be facing in the wrong direction.

not account for age-error differences in paleomagnetic poles, or the errors associated with the paleomagnetic studies (most commonly A95, Fisher, 1953).

Although the above approach is useful for testing a particular configuration between two landmasses at a particular point in time, a more robust test is to use apparent polar wander paths (APWP's) from multiple cratonic blocks. The assumption is that if two, or more, blocks are moving in unison, then they will trace out the same APWP. This is the approach used by Zhang et al. (2012) among others. A complete review is outside the scope of this summary article; however, except for a nearly unified "Nuna" core by at least 1700 Ma, there are vast differences in the myriad models of Columbia. Two examples (there are many) are shown in Fig. 7a,b (Zhang et al., 2012; Pisarevsky et al., 2014). Zhang et al. (2012) show a nearly unified Columbia whereas Pisarevsky et al. (2014) show a looser amalgam of continental blocks suggesting that Columbia was not yet fully assembled at 1700 Ma. One of the main issues in using APWP's for the Paleoproterozoic-Mesoproterozoic is that data are unevenly spaced in time and data coverage varies from craton to craton.

3. Statistical evaluation of paleomagnetic poles

3.1. Methods of analysis

One way to deal with the unevenly distributed paleomagnetic data is to start with an assumed configuration for Columbia and evaluate the fit for distinct time intervals. For example, Elming et al. (2021) assume a Columbia reconstruction valid from 1630 Ma to 1350 Ma. Because the density of paleomagnetic data were unevenly spaced in time, Elming et al. (2021) created snapshots of Columbia at 1630 Ma, 1490 Ma and 1350 Ma. The relative fits between the blocks remained fixed and paleomagnetic poles were rotated into the proposed configuration relative to the spin axis. Any departure from the ideal represents errors in either orientation or latitude of the proposed fit. Each reconstruction was shown along with the relevant paleomagnetic poles. "Goodness" of fit was not quantified in those reconstructions. A comparison between the closest approach technique and that used by Elming et al. (2021) is shown in Fig. 8a,b.

For much younger intervals, where paleomagnetic data are more abundant, there is controversy about how to evaluate the statistical difference from a reference direction (GAD), another pole, or location along an apparent polar wander path (GAPWP; Rowley, 2019; Heslop and Roberts, 2019; Vaes et al., 2022). Simple statistical measures are sometimes used to reject a particular result such as using the combined uncertainties between a reference pole and the pole being investigated. If the paleomagnetic pole falls outside of this error envelope:

$$CU = \sqrt[2]{A95_{ref}^2 + A95_{pp}^2}; \quad (1)$$

where ($A95_{ref}$ = reference pole and $A95_{pp}$ = paleomagnetic pole being evaluated), the pole is rejected (see Heslop and Roberts, 2019; Rowley, 2019). For comparing n-poles this equation can be expanded to:

$$\sqrt[2]{(A95_1)^2 + (A95_2)^2 + \cdots (A95_n)^2}; \quad (2)$$

These equations make several assumptions about the underlying data; (1) that the age difference between the poles is small enough such that significant plate motion has not occurred; (2) that the data are Fisherian and (3) secular variation is averaged out. Heslop and Roberts (2019) provide a Bayesian statistical approach to the problem with the same underlying assumptions. Other 'tests' for goodness of fit were developed by Watson (1956), Gordon and Cox (1980), McFadden and Lowes (1981), Bazhenov et al. (2016). Palencia-Ortas et al. (2011) used a variation of McFadden and McElhinny (1990) reversals test to grade pole comparisons A, B, C, Indeterminate or negative based on a comparison between the observed angular distance (γ_o) between means and the critical angle γ_c.

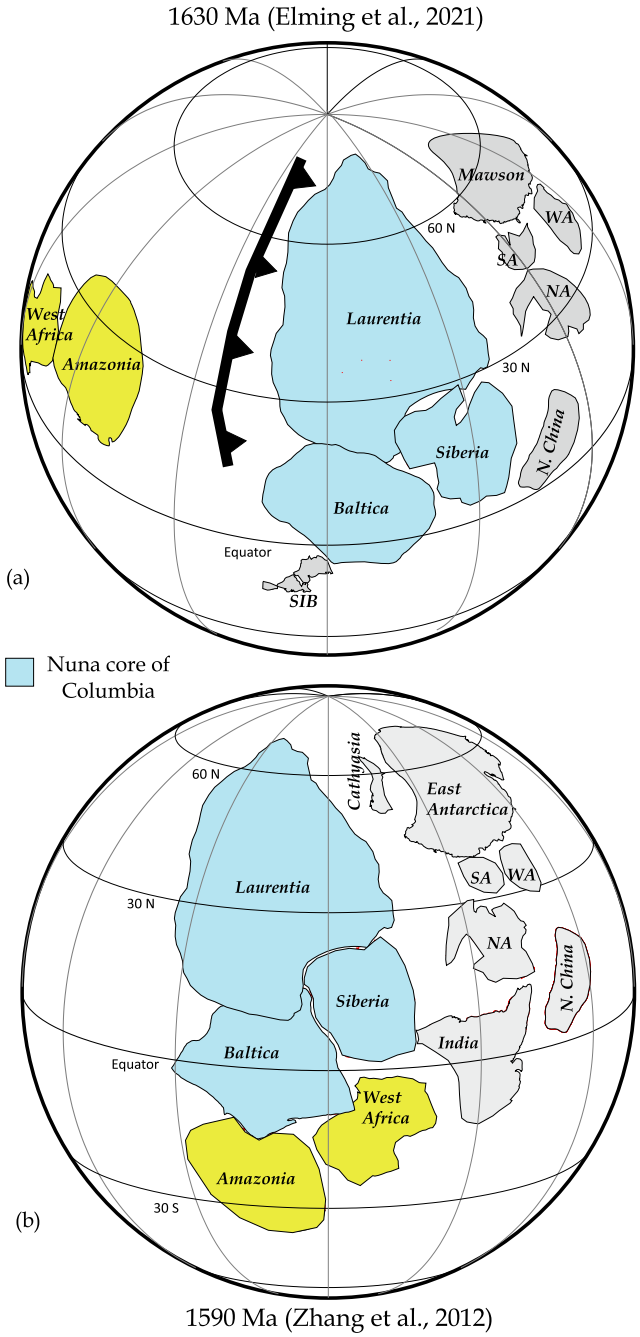

Fig. 7. Two alternative Columbia models at (a) 1630 Ma according to Elming et al. (2021) "No SAMBA" and (b) according to Zhang et al. (2012) with a SAMBA fit.

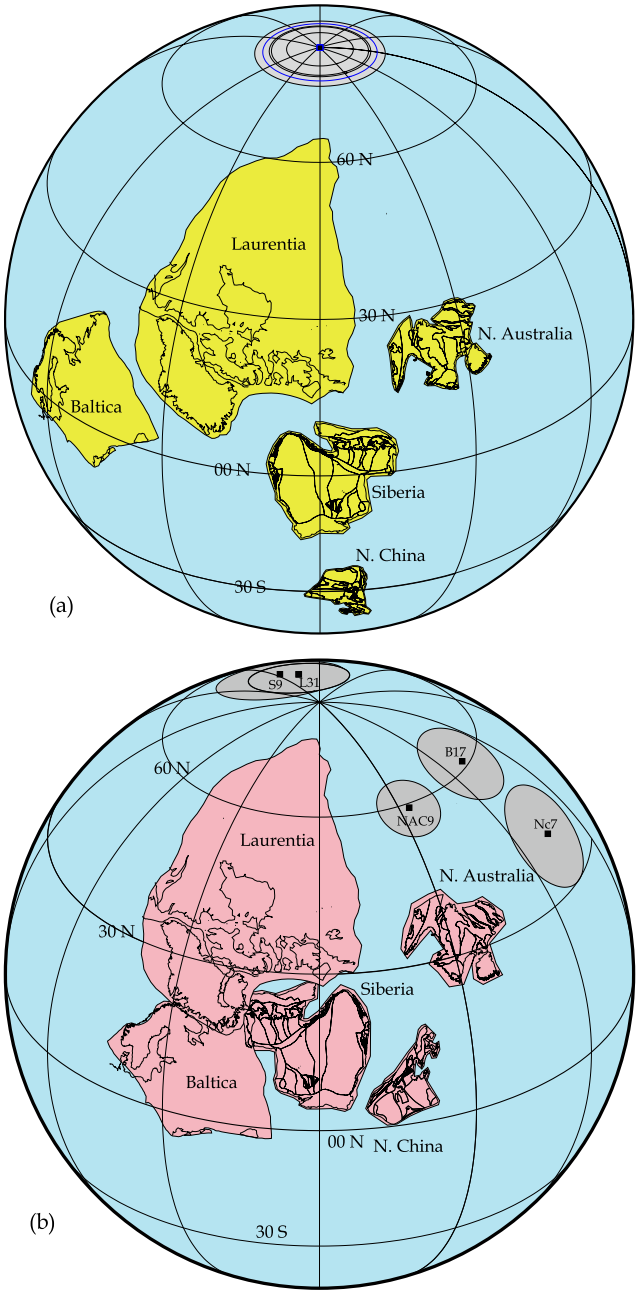

Fig. 8. (a) Paleogeographic reconstruction at 1630 Ma using the 'closest approach' technique. Age differences are ignored, and continents are positioned in an Elming et al. (2021) like configuration without overlap. All paleomagnetic poles are aligned with the spin axis; (b) Continents positioned in the Elming et al. (2021) Columbia fit, and poles are rotated according to the hypothesized configuration without regard to age differences.

The Proterozoic database is sparse and punctuated by large gaps in data such that most apparent polar wander paths consist of small segments for limited time intervals. Polar wander paths are expanded by assuming that two (or more) cratonic elements comprised the same plate and therefore poles from one are valid for all. It is quite rare to find multiple cratons with Precambrian poles that are dated to within +/- 10 Ma of each other. In addition, poles in the current database are sometimes calculated using mean declination and inclination (a_{95}) and other times using mean of virtual geomagnetic poles (VGP's; A95). Furthermore, there is no reference path, such as GAPWaP (Torsvik et al., 2012), for either Columbia or Rodinia. We use an approach combining Palencia-Ortas (2011), Heslop and Roberts (2019) and Rowley (2019) with some modifications to account for the irregular nature of the Proterozoic database.

We have recalculated the most reliable paleomagnetic data for the Columbia interval (see Elming et al., 2021) using pole statistics and corrected small errors in publications or databases. Where possible, we use means of VGP's and associated statistical measures (K, A95 and R). In a few cases, site mean directions or other details were not provided in the original publication and we use those data as reported and convert them as needed. We apply the following techniques to assess goodness of fit for paleomagnetic reconstructions.

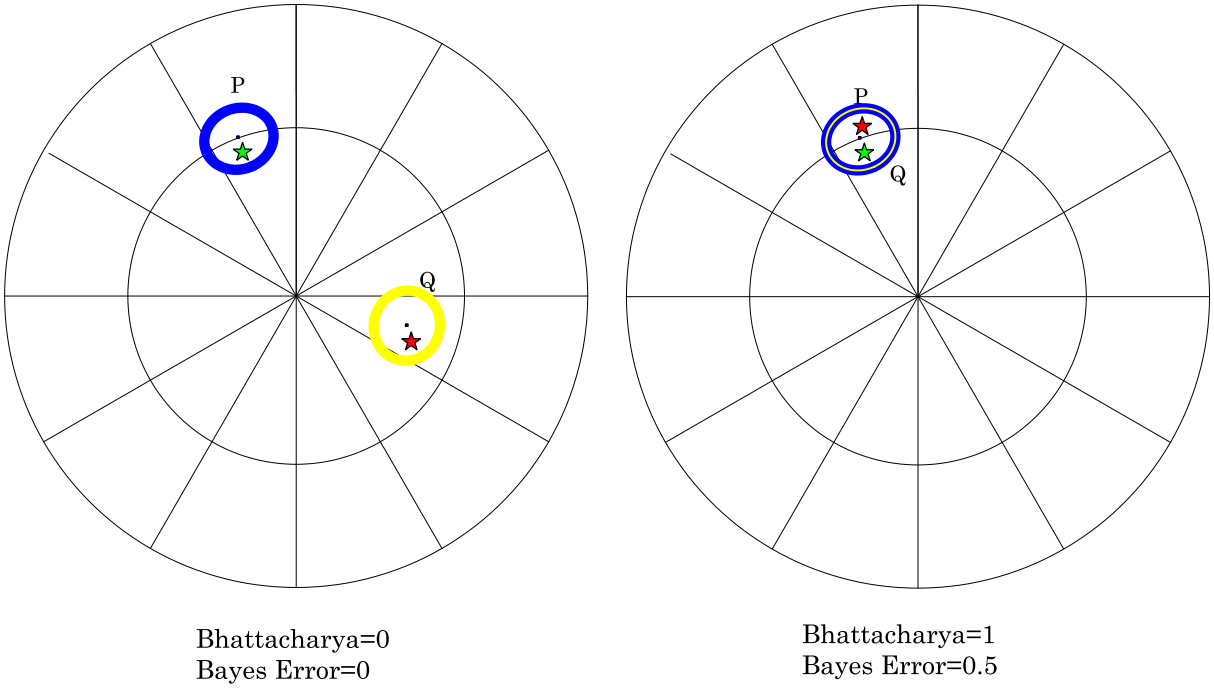

Fig. 9. (a) Two statistically different populations P and Q and their A95 envelopes (Bhattacharyya coefficient = 0.0). Two random observations are shown by a green star and red star. The probability of misclassifying the green star to population Q is 0 as is the probability of misclassifying the red star to population R (Bayes error = 0). (b) Two statistically identical populations P and Q along with their A95 envelopes (Bhattacharyya coefficient = 1). The probability of misclassifying the random green star to population Q is 50% or, conversely the red star to population P is 50% (Bayes error = 0.5). (For interpretation of the references to colour in this figure legend, the reader is referred to the web version of this article.)

Table 2
1780 Ma SAMBA Reconstruction.

Pole	N	R_f	Plat	Plong	A95	K	Plat(rot)**	Plong(rot)**	Age +/- (Ma)	R	Ref
Baltica											
B4-Notträsk	6	5	43.5° N	216.2° E	6.0°	124	82.1° N	197.8° E	1806 ± 6	5.96	1[a]
B5-Lake Ladoga	4	6	50.9° N	229.1° E	7.2°	146	86.3° N	37.5° E	1802 ± 17	3.98	2
B6-Kallax	5	5	49° N	209° E	3.9°	226	79.1° N	154.8° E	1796 ± 2; 1802 ± 3 (*1799*)	4.99	3
B7-Hoting	5	6	45.4° N	240.5° E	12.5°	38	82.7° N	305.2° E	1786 ± 10	4.9	4[a]
B8-Småland	11	7	45.7° N	182.7° E	8°	33.9	61.1° N	154.4° E	1780 ± 3; 1776 + 8/-7 *(1778)*	10.7	5
B9-Shoksa	36	6	39.7° N	221.1° E	5.5°	20	81.1° N	234° E	1775	34.2	6[b]
B10-Ropruchey	4	5	39.1° N	216.6° E	6.7°	109	79° N	217.3° E	1751 ± 3	3.99	7
Laurentia											
*L*11-Dubawnt	30	6	7° N	277° E	7.6°	12.2	77.7° N	299.7° E	1785 ± 4	27.6	8
ECMB	23	6	20.4° N	265.8° E	4.5°	45.6	84.4° N	153.7° E	1779.1 ± 2.3	22.5	9
L13-Jan Lake-A	10	3	28.1° N	268.9° E	17.2°	8.8	79.6° N	101.9° E	1758 ± 1; 1773 ± 9 (*1765.5*)	9	10[a]
L14-Cleaver	18	6	21.1° N	276.7° E	6.2°	31.9	83.8° N	33.3° E	1740 + 4/-5	17.5	11[a]
Amazonia											
AM3-Colider	10	5	63.3° N	119.9° E	10°	24.1	34.3° N	182.1° E	1789 ± 7	9.6	12
AM4-Avanavero	13	6	48.4° N	207.9° E	9.2°	19.8	81.6° N	187.9° E	1788.5 ± 2.5	12.4	13
Mean Age									1771.4 +/- 10		

Rotation Parameters (all to spin axis, + clockwise, -counterclockwise): Baltica: 34.5° N, 150.7° E, +51.5°; Laurentia: 0° N, 181.1° E, +72.1°;
Amazonia 62.0° N, 182.6° E, 119.9°. R_f = R-value Meert et al., 2020; Plat = Pole latitude; Plong = Pole longitude; A95 = cone of 95% confidence about the mean; Plat (rot) = rotated pole latitude; Plong(rot) = rotated pole longitude, R = length of the resultant vector (Fisher, 1953). Mean age based on weighted mean of ages for individual poles calculated in IsoPlotR (Vermeesch, 2018). References: 1[a]-recalculated from Elming, 1985; 2-Mertanen et al., 2006; 3-Elming, 1994; 4[a]-recalculated from Elming et al., 2009; 5-Pisarevsky and Bylund, 2010; 6[b]- K and R calculated using A95 from Pisarevsky and Sokolov, 2001; 7- Fedotova et al., 1999; Lubnina et al., 2012; 8- Park et al., 1973; 9- Swanson-Hysell et al., 2021; 10[a]- recalculated from Gala et al., 1995; 11[a]-recalculated from Irving et al., 2004; 12- Bispos-Santos et al., 2008; 13- Reis et al., 2013, Bispos-Santos et al., 2014.

Since it is rarely possible to compare identical age paleomagnetic poles in the Proterozoic, other sources of error should be considered. For example, if we compare two poles with a 20-million-year age gap, then it is reasonable to assume that both continents (and hence poles) underwent some displacement during that interval. Torsvik et al. (2012) calculated a mean apparent polar wander rate (APW) of 0.44°/Ma for the past 320 Ma which includes true polar wander (TPW) and continental motion (rotation and latitudinal motion). Torsvik et al. (2012) showed that total TPW during that same interval averaged to ~ 0 and therefore total APW was about 0.38°/Ma. Reliable estimates for APW rates in the Proterozoic are problematic. We apply the 0.44°/Ma estimate as a source of potential error in our comparisons. This amount is added to the combined uncertainty between two, or more, poles (Eqn. (3)). For

Table 3
1490 Ma Reconstruction (Elming et al., 2021).

Pole	N	R_f	Plat	Plong	A95	K	Plat(rot)**	Plong(rot)**	Age +/- (Ma)	R	Ref
Baltica											
B21-Ragunda	15	4	52.7° N	166.3° E	6.9°	32	52.8° N	132.2° E	1514 ± 5	14.6	1[a]
B22-Rødø	6	5	41.6° N	201.7°	9.5°	50	66.3° N	85.9° E	1497 ± 6	5.9	2[b]
B23-Tuna	4	4	28.3° N	179.8° E	13.2°	49	78° N	154.1° E	1474 ± 4; 1461 ± 1.2 (*1467.5*)	3.9	3[a]
B24-LakeLad	12	6	15.2° N	177.1° E	5.5°	63	77.2° N	219.5° E	1452 ± 12; 1459 ± 3; 1457 ± 2 (*1456*)	11.8	4[a]
Laurentia											
L16-SFM	17	6	−12.7° N	220.5° E	5.9°	38	69.5° N	281.3° E	1476 ± 16	16.6	5[a]
L17-Michikamau	12	6	−1.4° N	217.9° E	4.3°	104	74.3° N	246.5° E	1460 ± 5	11.9	6
L18-Spokane	8	6	−25.0° N	218.1° E	5.1°	119	57.9° N	292.1° E	1457 ± 12.5; 1468 ± 2 (*1462.5*)	7.94	7[a]
Siberia											
S10-Kuonomaka	5	4	−13.9° N	54.2° E	28.2°	8.3	50.2° N	237.2° E	1503 ± 3	4.5	8
S11-W. Anabar	21	6	−25.3° N	61.4° E	4.6°	49.5	57.8° N	255.3° E	1502 ± 2; 1503 ± 2 (*1502.5*)	20.6	9
S12-N. Anabar	9	5	−23.9° N	75.3° E	7.5°	48	70.5° N	257.1° E	1483 ± 17	8.8	10
S13-K-Sololi	13	6	−33.6° N	73.1° E	10.4°	17	65° N	279° E	1473 ± 24	12.3	11
India											
I4-Lakhna	8	5	−35.7° N	312.4°	15.5°	14	70.6° N	253.3° E	1466 ± 2.6	7.5	12[a]
North China											
NC8-Yangzhuang-P	11	6	2.8° N	190.1° E	15°	10.3	60.1° N	234.2° E	1437 ± 21; 1560 ± 5 (*1498.5*)	10.0	13[a]
NC9-Yangzhuang-W	15	6	17.5° N	214.4° E	6.6°	34	86.0° N	293.2° E	1437 ± 21; 1560 ± 5 (*1498.5*)	14.59	14
Sao Francisco											
SF1-Curaçá	6	6	10.5° N	10.2° E	19.2°	13.2	77.0° N	289.3° E	1507 ± 7	5.6	15[a]
								MEAN AGE	1463 +/- 8		

Rotation Parameters (all to rotation axis, + clockwise, -counterclockwise): Baltica: 47.5 N, 149.2 E, +116; Laurentia: −35.78 N, 5.3 E (**Note: Table 16.2 contains reporting error for Laurentia rotation which is corrected here.), −114.9; Siberia: 32.9 N, 121.5 E, −150.3; India: 11.5 N, 272.6 E, +150.5; North China: 41.7 N, 161.4 E, +97.8; Sao Francisco: 27.2 N, 318.1 E, +106.3. °. R_f = R-value Meert et al., 2020; Plat = Pole latitude; Plong = Pole longitude; A95 = cone of 95% confidence about the mean; Plat (rot) = rotated pole latitude; Plong(rot) = rotated pole longitude, R = length of the resultant vector (Fisher, 1953). Age of mean is calculated using weighted mean of ages for individual poles (IsoPlotR; Vermeesch, 2018). (*Mean age used in calculations*) References: 1[a] recalculated from Piper (1979); 2[b] Moakhar, 1998; 3[a] Mean of 4 poles Tuna, Bunkris, Glyson and Oje Nordic Paleomagnetic Working Group 2009 (Evans et al., 2021); 4[a] recalculated from Salminen and Pesonen (2007) and Lubnina et al. (2010); 5[a] recalculated from Meert and Stuckey, 2002 removed baked contact results; 6[a] Emslie et al., 1976 and Murthy et al., 1968; 7[a] recalculated from Elston et al., 2002; 8[a] recalculated from Ernst et al. (2008); 9,10 Evans et al. (2016); 11 Wingate et al., 2009; 12 Pisarevsky et al., 2013; 13 Pei et al. (2006); 14[a] Wu et al., (2005); 15[a]; recalculated from Salminen et al., 2016 removed baked contact means.

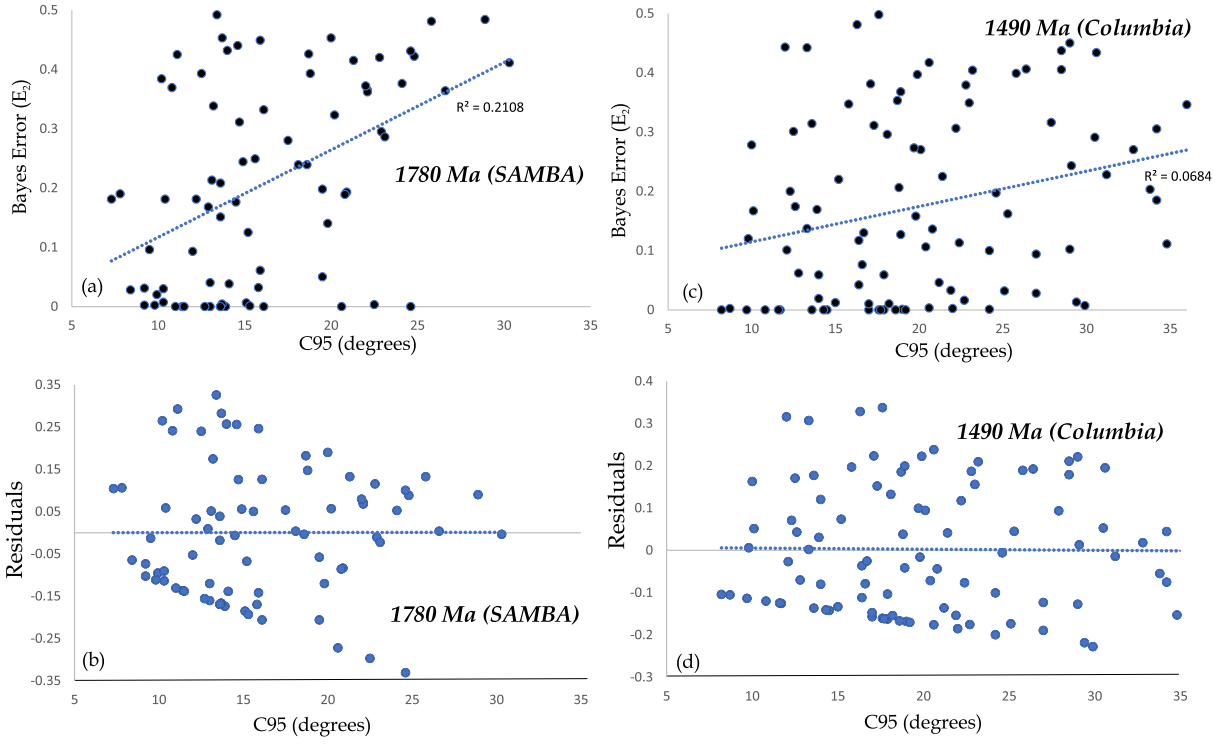

Fig. 10. (a) C95 versus Bayes error for paleomagnetic poles in Table 2 (1780 SAMBA) model; (b) Plot of residuals for the 1780 Ma regression; (c) C95 versus Bayes error for paleomagnetic poles in Table 3 (1490 Ma Columbia model); (d) Plot of residuals for the 1490 Ma regression. R^2-values indicate poor correlation between C95 and Bayes error.

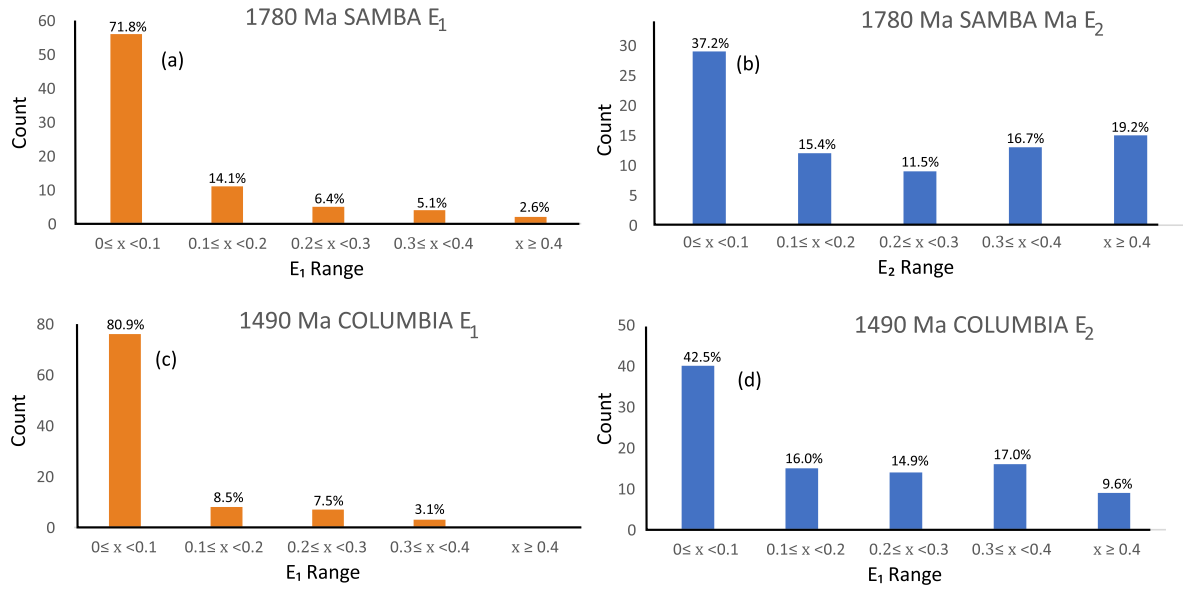

Fig. 11. (a) Binned E-values for 1780 SAMBA model without C95 errors; (b) Binned E-values for the 1780 SAMBA model with C95 errors; (c) Binned E-values for the 1490 Ma Columbia model without C95 errors and (d) Binned E-values for the 1490 Ma Columbia model with C95 errors.

example, if the poles have an age separation (ΔT) of 10 Ma, then 4.4° is added to the uncertainty of both poles (P_1 and P_2) to calculate the combined uncertainty **C95**:

$$\boldsymbol{C}95 = \sqrt{A95_{P1}^2 + A95_{P2}^2 + (0.44 * \Delta T)^2} \quad (3)$$

The combined uncertainty C95 is then used to calculate a new (pseudo) resultant vector length R_p and (pseudo) precision parameter (K_p) where:

$$R_p = \frac{\left[20^{\frac{1}{N-1}} - 1\right]N}{20^{\frac{1}{N-1}} - \cos(C95)}; \quad (4)$$

and the pseudo precision parameter (K_p) is given as:

$$K_p = \frac{(N-1)}{(N-R_p)}; \quad (5)$$

The values of R_p and K_p are then used to calculate the Bhattacharya coefficient (B) and Bayes error (E) using methods outlined in Heslop and Roberts (2019). The Bhattacharya coefficient has a maximum value of 1.0 (identical) and a minimum of 0 (completely dissimilar) and the Bayes error applies a continuous probabilistic value where E = 0.5 (maximum, distributions identical such that probability of misclassifying a random observation to the wrong population is 50%) or E = 0 (dissimilar, no chance of misclassification; Fig. 9a,b).

3.2. Tests of 1780 Ma SAMBA and 1490 Ma Columbia models

We use the 1780 Ma and 1490 Ma reconstructions of Elming et al. (2021) as examples because they allow for 78 and 94 binary comparisons between poles (see Tables 2, 3 and supplementary Table S-1 and S-2). Our analysis expands the error envelope (C95) around each pair of paleomagnetic poles to account for the individual uncertainties and the age differences between the poles. We then use that expanded error (C95) to evaluate each reconstruction using the Bayesian approach of Heslop and Roberts (2019). Larger C95 envelopes will, *ceteris paribus*, result in increasing agreement between potentially disparate poles and potentially limit the effectiveness of our proposed test. We plot C95 versus Bayes error (E_2) after age correction for all pole pairs in the 1780 Ma SAMBA and 1490 Columbia model of Elming et al. (2021) to test the correlation (Fig. 10). Although a general trend is evident in the expected direction, there is poor correlation between C95 and E_2 when C95 $\leq$ 30°. Therefore, we believe that our test provides some measure of goodness of fit for paleomagnetic reconstructions in the Proterozoic where age differences between individual poles used in reconstructions may vary by up to 60 Ma. We note that any poles that are statistically indistinguishable before C95 adjustment remain so. We have evaluated the B/E values for a SAMBA reconstruction at ~ 1.78 Ga and a Columbia reconstruction at ~ 1.49 Ga (Tables 2, 3). A binary comparison between each of the poles used in those reconstruction yields 78 comparisons (13 poles) at 1.79 Ga and 94 comparisons (15 poles) at 1.49 Ga (supplementary tables S-1 and S-2). In the 1780 Ma SAMBA test, the poles range in age from 1806 to 1740 Ma. Fig. 11a-d show the binned E-values for each pole comparison with/without using the C95 modification. The majority (~86%) of pole-to-pole comparisons in that reconstruction yield less than a 20% chance of misclassification (Bayes error) when not considering age differences. That number drops to ~ 53% of pole-to-pole comparisons when C95 is considered. The same is true for the 1490 Ma Columbia reconstruction of Elming et al. (2021) where ~ 90% of poles yield less than a 20% chance of misclassification which is lowered to 59% after C95 modification.

R_p was also used in a modification of the scheme proposed by Palencia-Ortas et al. (2011) for testing similarity of paleomagnetic poles according to the McFadden and McElhinny (1990) grading system for the reversal test using γ_c, where;

$$\gamma_c = \frac{(N - R_1 - R_2)(R_1 R_2)}{R_1 R_2} * \left[20^{\frac{1}{N-2}} - 1\right] \quad (6)$$

for p =.05. The pole similarity tests are graded A,B,C and Indeterminate for positive results or negative depending based on the magnitude of the critical angle (γ_c) to the observed angle (γ_o) between means. The McFadden and McElhinny (1990) test was applied using both published and pseudo R_p values. We used simulation in cases where poles did not have common kappa values (pre-C95 correction only). We evaluated pole pairs using both Bayesian and the MM1990 methods using pole parameters both with and without

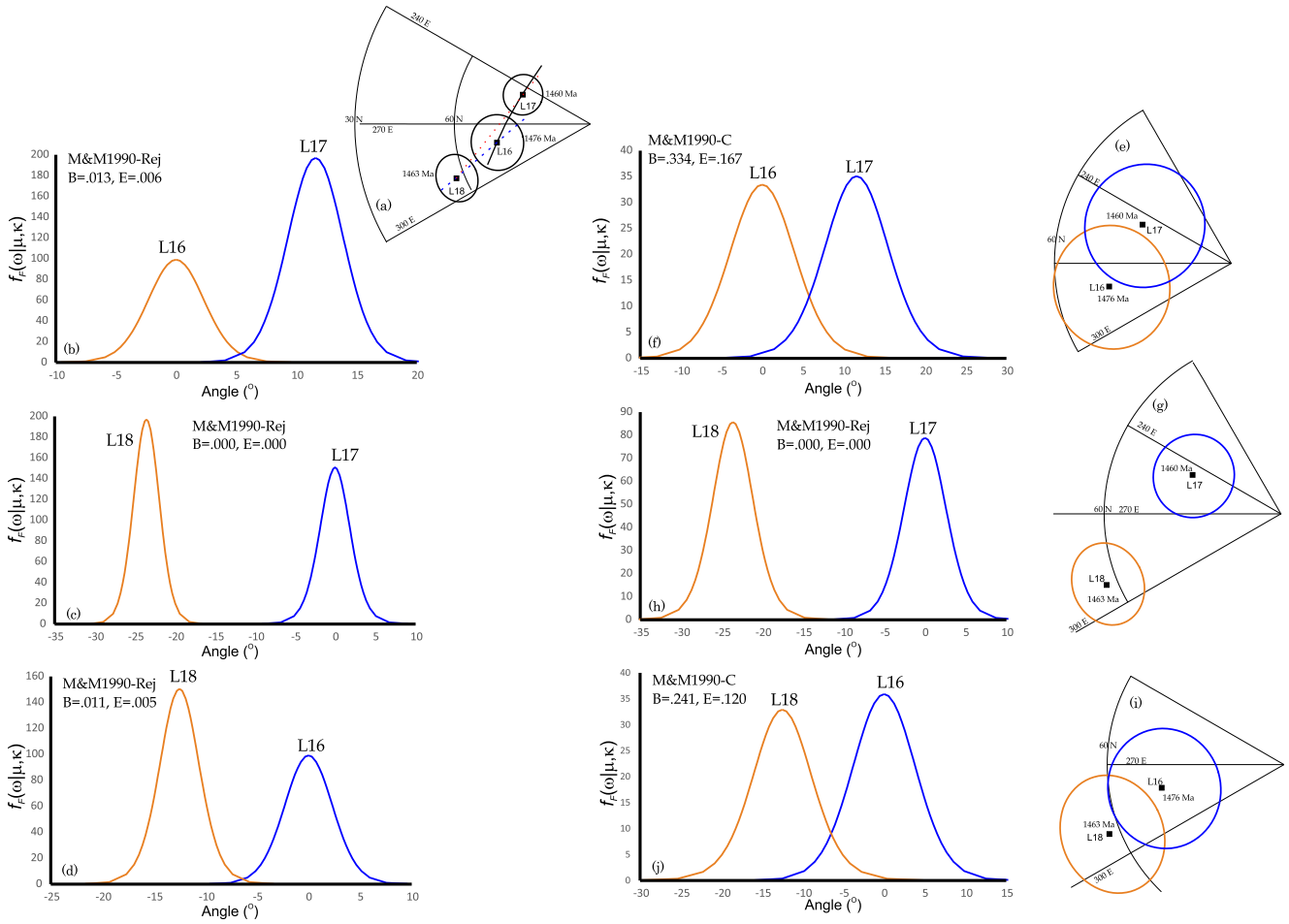

Fig. 12. (a) Paleomagnetic poles from the 1490 Ma Columbia reconstruction of Elming et al. (2021) for Laurentia with their A95 envelopes (see Table 3). Great-circle distances between the two poles are indicated by solid black line between L16 and L17; dashed blue line between L16 and L18 and dotted red line between L17 and L18 (b) probability density function calculated along the great-circle between pole L16 and pole L17 centered on L16; (c) probability density function calculated along the great-circle between poles L17 and L18 centered on L18; (d) probability density function calculated along the great-circle between poles L16 and L18 centered on L16; (e) C95 envelopes for L16 (orange) and L17 (blue); (f) probability density function for L16 and L17 using C95 centered on L16; (g) C95 envelopes for L18 (orange) and L17 (blue); (h) probability density function for L17 and L18 using C95 centered on L17; (i) C95 envelopes for L16 (blue) and L18 (orange); (j) probability density function for L16 and L18 using C95 centered on L16. (For interpretation of the references to colour in this figure legend, the reader is referred to the web version of this article.)

C95 for 1780 Ma SAMBA fit and 1490 Ma Columbia fits (Supplementary Tables S-1 and S-2).

3.3. Probability density functions

Heslop and Roberts (2019) illustrate differences between paleomagnetic poles by using the Fisher (1953) probability density function $f_F(\omega|\mu,\kappa)$:

$$f_F(\omega|\mu,\kappa) = \frac{\kappa}{4\pi \sinh(\kappa)} exp^{\kappa\mu^T\omega} \quad (7)$$

where κ = concentration parameter, $\mu^T\omega$ is the vector transpose between the unit vector representing the mean (μ) and ω (unit vector at some distance along a great-circle from the mean vector). Equation (7) is multiplied by R to obtain the maximum value for the pdf (when $\mu^T\omega = 1$). The pdf decays according to the spherical normal distribution (Fisher, 1953).

Fig. 12 illustrates pdf's for three Laurentian paleomagnetic poles from the 1490 Ma Columbia fit of Elming et al. (2021; Fig. 12a; Table 3). Fig. 12 b,c,d show the pdf functions for each of the three poles compared to each other using only K and R values. The MM90 test indicates a negative test for each pair. The Bhattacharyya coefficient (B) ranges between 0 and 0.013 and the Bayes error (E_2) is between 0 and 0.006 indicating poor correlation between the poles (Table S-2). The total age difference between the poles is only 16 Ma and an attempt to draw an APWP between the poles would require the path to oscillate past L16 (Fig. 12a). Fig. 12e-i illustrate the C95 error envelopes surrounding each of the poles and the pdf's are plotted along a great-circle connecting the two poles. Using K_p and R_p values, the MM90 test for L16 versus L17 and L18 versus L16 yield C grades. L18 and L17 yield a negative test due to non-overlapping C95 envelopes. The Bhattacharyya coefficients (B) for the two MM90 C-grade test cases range from 0.241 to 0.334 and the Bayes errors (E_2) are between 0.120 and 0.167. As noted by Heslop and Roberts (2019) there is no 'cut-off' value for making a reject/accept decision based on these values; however, the Bayes errors indicate only a 12–17% chance for misclassification whereas the binary MM90 test or 'visual overlap' would conclude the poles are indistinguishable.

We use these metrics in the following discussion of proposed Columbia supercontinent and other models as a first step in providing a more rigorous approach to evaluation Precambrian supercontinent configurations. We do not provide a binary accept/reject criteria for the Bayes error, but argue reconstructions dominated

Table 4
1550 Ma SAMBA Reconstruction.

Pole	N	R_f	Plat	Plong	A95	K	Plat(rot)**	Plong(rot)**	Age +/- (Ma)	R	Ref
Baltica											
B19-Satakunta	19	7	29.3° N	188.1° E	6.6°	26.6	80.6° N	132.1° E	1565 ± 35	18.3	1[a]
B20- Aland	76	7	24.2° N	192.9° E	3.3°	24.9	81.8° N	176° E	1572.9 ± 4.1	73	2[a]
Laurentia											
L15-Western Channel Diabase	35	5	9° N	245.5° E	4.3°	32.3	90° N	0° E	1591 ± 3.5	33.9	3[a]
Amazonia											
AM5-Mucajaí Complex	15	6	38.2° N	180° E	12.6°	10.2	72.7° N	282.5° E	1526.5 ± 2.0	13.6	4
								Mean Age	1547.1 ± 51		

Rotation Parameters (all to rotation axis, + clockwise, -counterclockwise): Baltica: 16.5° N, 118.7° E, +62.5°; Laurentia: 0° N, 155.5° E, 81°;
Amazonia 68.2° N, 140.7° E, +106.11°. R_f = R-value Meert et al., 2020; Plat = Pole latitude; Plong = Pole longitude; A95 = cone of 95% confidence about the mean; Plat (rot) = rotated pole latitude; Plong(rot) = rotated pole longitude, R = length of the resultant vector (Fisher, 1953). Age of mean is calculated using weighted mean of ages for individual poles (IsoPlotR; Vermeesch, 2018). 1[a]recalculated from Salminen et al. (2014);2[a]recalculated from Salminen et al. 2015); 3[a]recalculated using VGP means Irving et al., 1972; 4 Bispos-Santos et al., 2020. Note: SAMBA rotation parameters.

Table 5
1430 Ma SAMBA Reconstruction.

Pole	N	R_f	Plat	Plong	A95	K	Plat(rot)**	Plong(rot)**	Age +/- (Ma)	R	Ref
Baltica											
B24-Lake Ladoga	19	7	12.8° N	173.2° E	3.9°	58	74.3° N	004° E	1457 ± 3	18.4	1*
Laurentia											
L22-RMI	58	5	−12.2° N	216.9° E	3.1°	37	81.6° N	275.3° E	1433.8 ± 2.7	56.5	2[a]
L23-Mistatin	7	3	−1.0° N	201.5° E	7.6°	64	79.2° N	72.9° E	1420	6.9	3[a]
L24-McNamara	10	7	−14.3° N	210.2° E	7.9°	38	84.5° N	220.2° E	1401 ± 6	9.8	4[a]
Amazonia											
AM6-Nova G	19	6	47.9° N	65.9° E	7.0°	24	54.8° N	81.2° E	1418 ± 3.5	18.2	5
AM7-Indiavaí	16	3	57° N	69.8° E	8.6°	20	58.1° N	65.6° E	1415.9 ± 6.9	15.2	6
SCS-A2	18	6	56° N	98.5° E	7.9°	20	73.3° N	55.3° E	1440	17.1	7
RBS-A1	14	4	45.5° N	90.0° E	6.5°	39	70.6° N	93.0° E	1415.9 ± 6.9	13.7	8
								Mean Age	**1432.5 ± 9.8**		

Rotation Parameters (all to rotation axis, + clockwise, -counterclockwise): Baltica: 0.8° N, 86° E, +92.8°; Laurentia: 0° N, 299° E, −98.9°;
Amazonia 56.4° N, 66.7° E, +88.8°. R_f = R-value Meert et al., 2020; Plat = Pole latitude; Plong = Pole longitude; A95 = cone of 95% confidence about the mean; Plat (rot) = rotated pole latitude; Plong(rot) = rotated pole longitude, R = length of the resultant vector (Fisher, 1953). Age of mean is calculated using weighted mean of ages for individual poles (IsoPlotR; Vermeesch, 2018). Note that we have used the opposite polarity for Amazonian poles compared to Elming et al., 2021. 1*Differs from Lake Ladoga result in Elming et al. (2021). Our mean is based on VGP's reported by Lubnina et al. (2010) and Salminen and Pesonen (2007).; 2[a] recalculated from Harlan et al., 1994 and Harlan and Geissman, 1998; 3[a] recalculated from Fahrig and Jones, (1976); 4[a] recalculated from Elston et al., 2002.; 5 Bispos-Santos et al. (2012); 6 D'Agrella-Filho et al., 2012; 7,8; D'Agrella-Filho et al. (2016). SCS = Salto de Céu; RBS = Rio Branco Sediments.

Table 6
1380 Ma SAMBA Reconstruction.

Pole	N	R_f	Plat	Plong	A95	K	Plat(rot)**	Plong(rot)**	Age +/- (Ma)	R	Ref
Baltica											
B25-S. Urals	5	5	2.0° N	188.5° E	10.3°	56	78.3° N	331.2° E	1381.5 ± 15.4	4.9	1[a]
Laurentia											
L24-McNamara	10	7	−13.5° N	208.3° E	6.7°	39	84.2° N	294.1° E	1401 ± 6	9.8	2[a]
L25-Pil-Lib	4	6	−20.6° N	215.1° E	8.0°	132	77.9° N	337.7° E	1365 ± 3	3.99	2[a]
G-L32 Victoria Fjord	9	5	12.2° N	243.9° E	4.6°	125	54.2° N	358.3° E	1382 ± 2	8.9	3[a]
G-L33-Midsommersø	10	5	7.5° N	254.2° E	5.2°	87	59.7° N	356.4° E	1382 ± 2	9.9	4[a]
G-L34-Zig-Zag	19	5	14.2° N	231.2° E	3.1°	76	54.7° N	360.0° E	1382 ± 2	18.8	4[a]
Amazonia											
AM6-Nova Guarita	19	6	47.9° N	65.9° E	7.0°	24	46.6° N	80.8° E	1418 ± 3.5	18.2	5
AM7-Indiavai	16	3	57° N	69.7° E	8.9°	20	49.1° N	67.2° E	1415.9 ± 6.9	15.2	6
									1387 +/- 14.9		

Rotation Parameters (+clockwise, -counterclockwise): Baltica: 0.96° N, 271.7° E, −98.2°; Laurentia: 0° N, 302.6°, −107.5° E (mean of L24 and L25); Greenland: 6.8° N, 307.2° E, −110.6°; Amazonia 52.2° N, 74.4° E, 94.1°. R_f = R-value Meert et al., 2020; Plat = Pole latitude; Plong = Pole longitude; A95 = cone of 95% confidence about the mean; Plat (rot) = rotated pole latitude; Plong(rot) = rotated pole longitude, R = length of the resultant vector (Fisher, 1953). Age of mean is calculated using weighted mean of ages for individual poles (IsoPlotR; Vermeesch, 2018). References: 1[a] recalculated from Lubnina, 2009; 2[a] recalculated from Elston et al., 2002; 3[a] recalculated from Abrahamsen and Van der Voo, 1987; 4[a] recalculated from Marcussen and Abrahamsen, 1983; 5[a] recalculated from Bispos-Santos et al., 2012; 6 D'Agrella-Filho et al., 2012.

by lower E-values (<0.2) should be reviewed closely for potential sources of error and viewed with caution. We note that we are using this method to test specific reconstructions with defined rotation parameters. Changing rotations parameters, combining multiple (different age) poles into a grand mean pole, or eliminating poles that do not fit may yield 'better' results, but pole-by-pole comparisons should be the preferred approach.

4. Discussion: Summary of Columbia reconstructions

4.1. Great Proterozoic Accretionary Orogen & SAMBA within Columbia

Condie (2013) amongst others made note of the predominance of accretionary orogenic belts associated with the Columbia supercontinent. Johansson (2009) proposed a link between Amazonia

and Baltica (SAMBA; Fig. 4) that was perceived as a nearly one-billion-year connection (~1.8–0.8 Ga) between these two cratons whose outboard margins were the locus of accretion. By default, the close connections between Baltica and Laurentia during the Mesoproterozoic meant that Laurentia is included as the third continent in SAMBA. The SAMBA connection is controversial. For example, Pisarevsky et al. (2014) argues that Amazonia was never incorporated into Columbia whereas D'Agrella-Filho et al. (2021) conclude that the SAMBA connection is valid from ~ 1.8–1.4 Ga. Studies in the Svecofennian province indicate a late-stage continent–continent collision in the Paleoproterozoic (Korja and Heikkinen, 2005). In the original studies, the continent was not identified but after the SAMBA proposal, Amazonia was named as the presumptive, but not definitive, candidate (Korja et al., 2006; Korja and Heikkinen, 2008; Roberts and Slagstad, 2014; Almeida et al.,2021).

Paleomagnetic data form the crux of many arguments for and against SAMBA. Paleomagnetic tests require coeval data from both Baltica and Amazonia, but we argue that Laurentia should also be included in this analysis. Unfortunately, these data are limited to narrow time intervals and the results are ambiguous. We examine the proposed SAMBA model at 1.78, 1.55, 1.42 and 1.35 Ga. Individual poles and rotation parameters are listed in Tables 2, 4–6.

As previously noted, the majority of the paleomagnetic poles for SAMBA at 1.78 Ga indicate a low probability of misclassification and hence poor fit to the model. Even when C95 modified, the SAMBA model is a 50–50 proposition on a pole-to-pole comparison (Supplementary Table S-1). The Avanavero pole (AM4) yields a reasonable fit between most of the other poles except for the Colider (Amazonia), Dubawnt (Laurentia) and Smäland (Baltica) poles. The Avanavero is the pole of choice for the proposed SAMBA fit and was used by D'Agrella-Filho et al (2021) to argue in favor of a long-term linkage between Amazonia and Baltica (see also Zhang et al., 2012; Bispos-Santos et al., 2014). In contrast Elming et al. (2021) argue against the SAMBA connection and leave Amazonia out of the Columbia supercontinent based in part on the poor fit between the Colider (AM5) pole in the SAMBA reconstruction and misfits at younger times (also see arguments by Pisarevsky et al., 2014). The discrepancy between the two 1.78 Ga poles from Amazonia cannot be remedied by a simple rotation as the latitudinal separation is ~ 30°. Bispos-Santos et al. (2014) offered a solution by separating the SW Amazonian region from the Guiana shield at 1.78 Ga; however, there is little geological evidence to support this scenario.

The 1.55 Ga reconstruction is based on a much smaller dataset (Table 4) with a large spread in ages. If C95 errors are not used, the poles show little similarity to one another (Supplementary Table S-3) with E-values ranging from 0 to 0.138. A better correlation is achieved after C95 modification. There are many slight variations in proposed SAMBA reconstructions (see Bispos-Santos et al., 2020) and reasonable fits can be obtained using the data in Table 4 at 1.55 Ga.

The SAMBA connection was also tested at 1.43 and 1.38 Ga. The proposed SAMBA fit at 1.43 Ga (Table 5) is constrained by a single pole from Baltica. The Baltica pole does not compare well with any of the Amazonian poles with Bayes errors ranging between 0 and 0.154 (using C95 confidence intervals; Supplementary Table S-4). The Mistatin pluton (Laurentia) paleomagnetic pole compares better with the Salto de Céu and Rio Branco poles of Amazonia with C95 Bayes errors of 0.396 and 0.210. Overall, only 28% of paleomagnetic poles from the 1430 Ma ensemble have Bayes errors>0.20. At 1.38 Ga, the two poles from Amazonia are distinct from every pole from Baltica and Laurentia (with and without C95) such that the SAMBA fit can be rejected at that time (Table 6; Supplementary Table S-5).

Kulakov et al. (2022) present new late Mesoproterozoic to early Neoproterozoic data from Baltica which are incompatible with the SAMBA connection at 1.09 Ga. It is our tentative conclusion that the SAMBA connection, if valid, was much shorter lived than Johansson (2009) envisioned and is paleomagnetically permissible only from ~ 1.78–1.5 Ga and by rejecting one of the Amazonian poles. Rogers and Santosh (2002) made the case for rifting of Columbia sometime around 1.5–1.4 Ga and cited the widespread occurrence of A-type granites in North America, Amazonia and Baltica. At face value, this would agree with the limited paleomagnetic data outlined here. The nature and tectonic setting for A-type magmatism is controversial although a post-collisional extensional regime is consistent with ferroan granite generation (Bonin, 2007; Frost and Frost, 2011; DuBray et al., 2021). In contrast, Pisarevsky et al. (2014) and Elming et al. (2021) do not include Amazonia (nor West Africa) in the Columbia supercontinent.

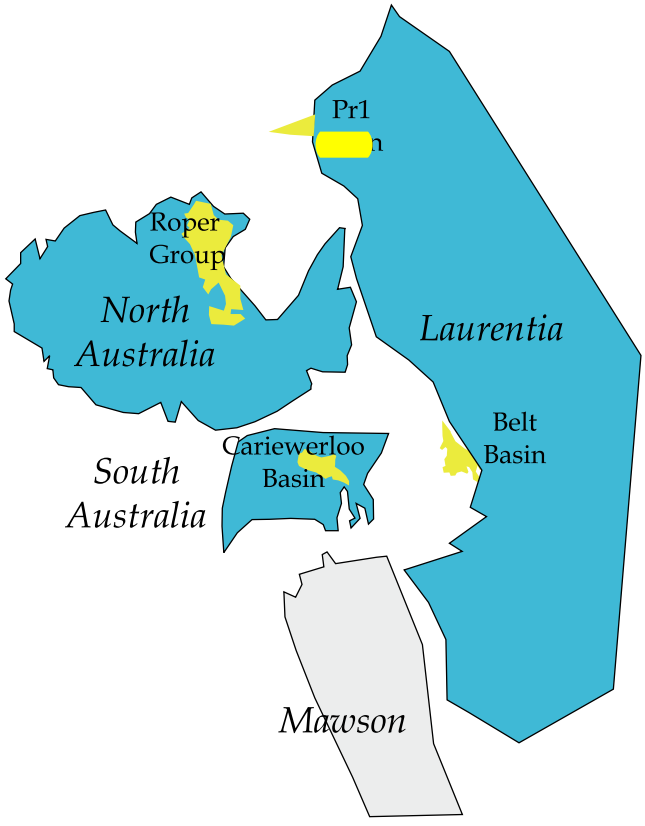

Fig. 13. Alternative fit of Northern Australia according to Morrisey et al. (2019).

4.2. Australia/Mawson craton in Columbia

Australia (Northern, South, and Western) along with the Mawson block of East Antarctica were originally placed in the SWEAT configuration in some early Columbia models (Zhao et al., 2002 after Moores, 1991). The implication of that position is that the SWEAT connection persisted from Columbia assembly until Rodinia breakup. The paleomagnetic database is limited for Australia during the lifespan of Columbia; however, subsequent studies propose a very similar 'proto-SWEAT' fit which places the Australian blocks adjacent to the NW margin (present-day coordinates) of Laurentia and close to the North China craton (Zhang et al., 2012; Elming et al., 2021; Kirscher et al., 2021a,b). Morrisey et al. (2019) place the combined Australia-Mawson blocks adjacent to western North America with the Cariewerloo Basin (South Australia) alongside the Belt-Purcell Basin (Laurentia; Fig. 13). The principal argument in favor of this intermediate position is that

Table 7
1630 Ma Reconstruction (Elming et al., 2021).

Pole	N	R_f	Plat	Plong	A95	K	Plat(rot)**	Plong(rot)**	Age +/- (Ma)	R	Ref
Baltica											
B14-Häme	11	5	23.9° N	208.9° E	15.2°	10	73.6° N	302.3° E	1642 ± 4; 1647 ± 14 (*1644.5*)	9.99	1[a]
B15-Sipoo	5	4	26.4° N	180.4° E	7.4°	108	62.8° N	233.5° E	1633 ± 10	4.96	2[a]
B16-Suomen	10	4	27.9° N	171.7° E	7.9°	38	57.2° N	222.3° E	1638 ± 32	9.76	3[a]
B17-Wiborg	9	3	30.6° N	175.1° E	8.9°	34	61.2° N	220.6° E	1617 ± 2; 1630 ± 9 (*1623.5*)	8.77	4[a]
B18-Hoting	4	4	12.2° N	182.0° E	6.7°	189	53.4° N	254.2° E	1614 ± 24	3.98	5
Laurentia											
L31-Melville	9	6	1.6° N	261.7° E	9.3°	31	76.2° N	346° E	1622 ± 3; 1629 ± 1; 1632 ± 1; 1635 ± 3 (*1629.5*)	8.74	6[a]
Siberia											
S9-Nersa	95	5	23° N	310° E	12.0°	2.5	73.9° N	356.8° E	1641 ± 24	56.7	7[b]
North Australia											
NAC7-Malla	3	6	−36.7° N	214.2° E	5.2°	572	71.8° N	44.4° E	1655 ± 10	2.99	8[b]
NAC8-Toog	72	7	−61° N	186.7° E	6.1°	8.5	76.5° N	263.2° E	1648 ± 3	63.6	8[b]
NAC9-Emmu	47	5	−79.1° N	202.6° E	6.1°	13	59.2° N	283.9° E	1644 ± 9	43.3	8[b]
NAC10-Balb	46	6	−66.1° N	177.5° E	4.6°	22	70.1° N	259.3° E	1609 ± 3; 1613 ± 4 (*1611*)	43.9	9[b]
North China											
NC7-Mengyin	9	5	19° N	181.3° E	10.5°	25	40.4° N	222.7° E	1634 ± 6	8.68	10[a]
Means									1629 +/- 8		

Rotation Parameters (all to rotation axis, + clockwise, -counterclockwise): Baltica: 57.4° N, 165.2° E, +102.7°; Laurentia: −35.76° N, 20.57° E, −97.97°; Siberia: 39.6° N, 132.4° E, −164.9°; North China: 51.4° N, 177.9° E, +82.1°; North Australia craton 14.5° N, 148.2° E, +149.9°. R_f = R-value Meert et al., 2020; Plat = Pole latitude; Plong = Pole longitude; A95 = cone of 95% confidence about the mean; Plat (rot) = rotated pole latitude; Plong(rot) = rotated pole longitude, R = length of the resultant vector (Fisher, 1953); Age of mean is calculated using weighted mean of ages for individual poles (IsoPlotR; Vermeesch, 2018). References: 1[a] recalculated from Salminen et al. (2017); 2[a] recalculated from Mertanen and Pesonen (1995); 3[a] recalculated from Salminen et al. (2019); 4[a] recalculated from Neuvonen (1986); 5 from Elming et al. (2009).; 6[a] recalculated from Halls et al. (2011);7[b] calculated from reported A95 and N, Metelkin et al. (2005); 8[b] calculated from reported A95 and K Idnurm et al. (1995); 9[b] calculated from A95 and K Idnurm (2000); 10[a] recalculated from Cai et al. (2020).

Table 8
1350 Ma Reconstruction (Elming et al., 2021).

Pole	N	R_f	Plat	Plong	A95	K	Plat(rot)**	Plong(rot)**	Age +/- (Ma)	R	Ref
Baltica											
B25-S. Urals	5	5	2.0° N	188.5° E	10.3°	56	72.7° N	23.5° E	1386 ± 5; 1366 ± 6; 1384 ± 3; 1386 ± 6 *(1381)*	4.9	1[a]
BD-Bornholm	27	6	4.5° N	166.1° E	6.5°	19	78.5° N	162.7° E	1326 ± 10	25.6	2[a]
Laurentia											
L24-McNamara	10	7	−14.3° N	210.2° E	7.9°	39	83.8° N	313.1° E	1401 ± 6	9.8	3[a]
L25-Pil-Lib	4	6	−20.6° N	215.1° E	8.0°	132	76.7° N	334.5° E	1365 ± 3; 1401 ± 6 *(1383)*	3.99	3[a]
L26-Nain	21	5	11.7° N	206.7° E	2.2°	163	69.9° N	145.7° E	1305 ± 15	20.9	4[a]
G-L33-Midsommersø	10	4	7.4° N	230.0° E	5.2°	89	65.1° N	83° E	1382 ± 2	9.9	5[a]
G-L34-ZigZag	19	4	12.6° N	231.2° E	3.1°	76	60.8° N	90° E	1382 ± 2	18.8	5[a]
Siberia*											
S15-Dzhogdzho	10	5	−24.9° N	55.5° E	10.4°	22.6	77.3° N	249.2° E	1397 ± 4	9.6	6[a]
Amazonia											
AM6-Nova Guarita	19	6	−47.9° N	225.9° E	7.0°	24	71.1° N	110.5° E	1418 ± 3.5	18.2	7[a]
AM7-Indiavai	16	3	−57° N	249.8° E	8.6°	20	79.3° N	91.7° E	1415.9 ± 6.9	15.2	8[a]
North China											
NC11	18	6	−5.9° N	179.6° E	4.3°	67	68.2° N	208.8° E	1320 ± 4; 1324 ± 5; 1325 ± 5 *(1323)*	17.7	9
Mean									1382 +/- 13		

Rotation Parameters (all to rotation axis, + clockwise, -counterclockwise): Baltica: 38.2° N, 139.6° E, +131°; Laurentia: −34.48° N, −7.25° E, −132.78°; Siberia: 25.5° N, 111.5° E, −137.2°; North China: 33.3° N, 151.6° E, +115.5°; Amazonia −6.54° N, 2.09° E, −160.3°. R_f = R-value Meert et al., 2020; Plat = Pole latitude; Plong = Pole longitude; A95 = cone of 95% confidence about the mean; Plat (rot) = rotated pole latitude; Plong(rot) = rotated pole longitude, R = length of the resultant vector (Fisher, 1953); Age of mean is calculated using weighted mean of ages for individual poles (IsoPlotR; Vermeesch, 2018). References: 1[a] Recalculated from Lubnina, 2009; 2; recalculated from Luoto et al., 2021; 3[a], recalculated from Elston et al., 2002;4[a] recalculated from Murthy, 1978; 5[a] recalculated from Marcussen and Abrahamsen, 1983; 6[a] recalculated from Veselovskiy et al., 2009; 7[a] recalculated from Bispos-Santos et al., 2012; 8[a] recalculated from D'Agrella-Filho et al., 2012; 9 Chen et al., 2013. *Chieress dyke VGP (1 site) included in Elming et al. (2021) table was not used in this analysis.

it aligns 1.45 Ga metamorphic and igneous belts of the Gawler craton with those in North America whereas the proto-SWEAT reconstruction results in significant offset. The assembly of this part of Columbia involves terrane transfer of the Georgetown inlier to Australia between 1650 and 1600 Ma after which both collided with Laurentian (Pourteau et al., 2018; Nordsvan et al., 2018).

Paleomagnetic evidence for Australia's position within Columbia is limited. Higher-quality poles are available only at 1611–1655 Ma (Table 7). We provide a test of the Elming (2021) Columbia model with North Australia in the 'proto-SWEAT' configuration. The Melville-Bugt dykes (Halls et al., 2011) from Laurentia is poorly correlated with all North Australian poles (E-values for C95 adjusted poles range from 0.036 to 0.130; Supplementary Table S-5) in the Elming et al. (2021) model. A more southerly position for these blocks is approximated by the AUSWUS fit (Karlstrom et al., 1999) and yields a better correlation with the Melville pole with E-values ranging from 0 to 0.411. There are no quality poles from Australia to test the Columbia fit at 1.49 and 1.35 Ga in the Elming et al. (2021) compilation.Table 8..

4.3. Siberian craton in Columbia

Siberia (Anabar, Angara and Aldan), together with Laurentia and Baltica form the Nuna core of the Columbia Supercontinent (Meert, 2012; Mitchell et al., 2021). Unfortunately, quality paleomagnetic data are limited to a total of 8 poles for the interval from 1.74 to 1.38 Ga. Six of the paleomagnetic poles are from the Anabar-Angara block and two from the Aldan. Moreover, two-thirds of

the paleomagnetic poles from the Anabar-Angara block are nearly the same age (between ~ 1.449–1.508 Ga) and have nearly overlapping error envelopes (Pisarevsky et al., 2021). Pisarevsky et al. (2021) discuss two options for a Siberia fit in Columbia along the Arctic margin of Laurentia. Pisarevsky et al. (2021) favor a 'loose fit' whereby Siberia and Laurentia occupy the same plate with the Yangtze craton sandwiched between Siberia and Laurentia. Others favor a tighter fit between Laurentia and Siberia (Evans and Mitchell, 2011).

A third option was favored by Sears and Price (1978, 2003) with Siberia along the present-day northwestern margin of Laurentia. The Sears and Price (1978) model is based upon numerous geological connections between the Laurentia-Siberia in the NW-fit but paleomagnetic data do not support their configuration. Sears (2022) offers a possible solution for the discrepancy between the paleomagnetic data and the proposed NW-Laurentia and Siberia links by arguing for a tesseral quadrupolar magnetic field that was semi-stable during the Proterozoic. The chosen field configuration does allow for the Sears and Price (1978, 2003) model but was not evaluated on a more global scale.

The Elming et al. (2021) model uses the tight fit of Siberia against the Arctic margin of Laurentia. A single pole from the Nersa complex is used to position Siberia at ~ 1630 Ma (Metelkin et al., 2005). Elming et al. (2021) cite an age of 1641 ± 8 Ma from Ernst et al. (2016) as representative of the Nersa paleomagnetic pole. However, numerous Late Neoproterozoic and early Paleozoic ^{40}-Ar/^{39}Ar ages are found in the same area including some of the paleomagnetic sampling sites (Sklyarov et al., 2003; Gladkochub et al., 2007; Vasyukova et al., 2019) raising questions about the uncritical use of this pole in Mesoproterozoic reconstructions. Therefore, although the proposed fit is supported by the Nersa paleomagnetic data, we urge caution until more data from the dated intrusions are provided.

The comparison between Siberia and Laurentia is more easily evaluated between 1.5 and 1.46 Ga as both Laurentia and Siberia have several high-quality paleomagnetic poles (Table 3; Supplementary Table S-2). These poles show reasonable agreement using C95 supporting the tight fit of Elming et al. (2021). At ~ 1.35 Ga, there is a single pole from Siberia (Veselovsky et al., 2009), one VGP from Siberia (Ernst et al., 2000) and 4 poles from Laurentia. The Chieress dyke VGP is well-dated but receives only an R_f = 2 (Meert et al., 2020). The Dzhogdzho-Kotyaka intrusions (Veselovsky et al., 2009) receive an R_f = 5, but lacks a well-defined age. We use the Dzhogdzho pole because the cluster of VGP's from that study encompass the Chieress dyke VGP. Based upon our review, only the McNamara pole (Elston et al., 2002) shows reasonable agreement with Siberia in the Elming et al. (2021) reconstruction whereas the nearly coeval Pilcher-Libby pole (Elston et al., 2002) does not. None of the Greenland poles (after rotating to Laurentia) show good agreement with Siberia.

The'loose-fit' model of Pisarevsky et al. (2021) does not fare better in a pole-by-pole comparison. Every Siberia-Laurentia pole comparison in the 1780 Ma and 1470 Ma compilation has E-values ranging from 0 to 0.071 before C95 comparison. The best fit after C95 consideration is between the Kuonamaka pole (A95 = 28°) and the St. Francois Mountains (SFM; Meert and Stuckey, 2002) pole which is 30 Ma younger. Comparisons between the SFM pole and the other three Siberian poles at 1470 Ma have E-values between 0 and 0.144.

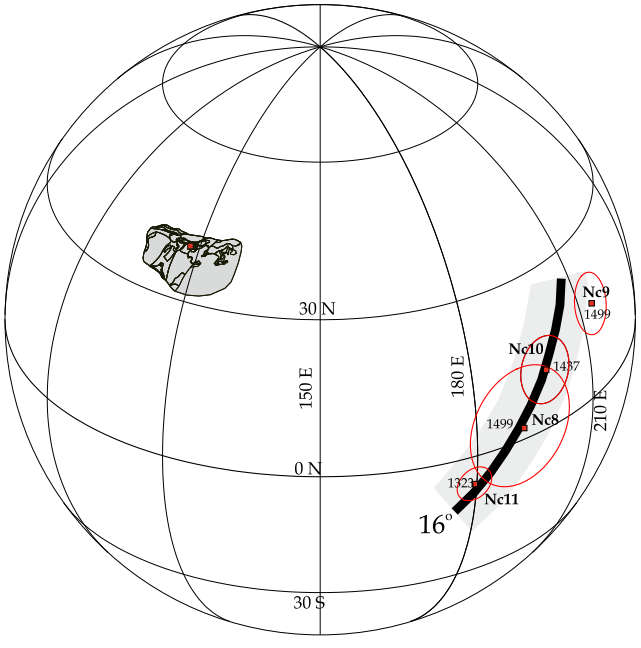

Fig. 14. North China Block poles NC7-10 (1323–1499 Ma) fall along a great-circle defining 16°latitude (Beijing reference location).

4.4. North China, India and Congo-São Francisco and Rio Plata cratons in Columbia

Paleomagnetic data from North China, India, Rio de la Plata and the Congo-São Francisco craton can also be evaluated for their location within the Columbia supercontinent although data are limited for India (2 poles), Congo-São Francisco (2 poles) and Rio de la Plata (1 pole).

The favored position for the North China craton within Columbia is adjacent to the Australian blocks along the margin of Columbia (Zhang et al., 2012; Pisarevsky et al., 2014; Elming et al., 2021; Zhang et al., 2021). Other positions were proposed for the North China Block based on geological correlations (Rogers and Santosh, 2002, 2009; Zhao et al., 2002, 2004) or alternative interpretations of the paleomagnetic data (Pesonen et al., 2012; Chaves and de Rezende, 2019). Due to limited data, the positions of India, Rio de la Plata and Congo-São Francisco are less well-constrained. In addition, Peninsular India was commonly treated as a unified block whereas current paleomagnetic and geological data indicate the North India and South India blocks should be treated separately during the Paleo-Mesoproterozoic (Meert et al., 2021).

The North China Block (NCB) has a dozen paleomagnetic results that were used by Elming et al. (2021) to evaluate its position in Columbia. Evans et al. (2021) ranked five of these as "A" poles. The biggest issue related to the NCB data is a lack of well-bracketed ages for some of the sedimentary sequences. For example, the original age of the Yangzhuang Formation (Jixian section) was assumed to be ~ 1.33 Ga (Pei et al., 2006). Subsequent U-Pb zircon ages bracket the sedimentation between 1.44 and 1.56 Ga with a nominal assumed age of 1.5 Ga for the Yangzhuang (Huakin, et al., 2014; Evans et al., 2021). There are several poorly defined ^{40}Ar/^{39}Ar isochron ages from the same sequence (Wang et al., 1995) that led Pei et al. (2006) to cite an age of 1.35 Ga for the pole. The ~ 1.5 Ga pole passes a fold and reversals test but also closely resembles the 1323 Ma Yanliao mafic sills pole (Chen et al., 2013). All poles between 1499 and 1323 Ma from the NCB lie along the same small circle arc indicating only small differences in declination that might be produced from localized vertical axis rotations (Fig. 14).

Although the proposed reconstruction of the NCB in at 1.35 Ga appears to yield high E-values when compared to Laurentia, Siberia and Baltica poles, these result from large age differences (and correspondingly high C95 values). Paleomagnetic poles closer in age

to the Yanliao sill include the Bornholm dyke pole (Baltica; Luoto et al., 2021) and the Nain anorthosite pole (Murthy, 1978) with E-values of 0.018 and 0.006 respectively. Therefore, the proposed reconstruction of the NCB of Elming et al. (2021) is not supported by their data.

The Indian Proterozoic database is greatly expanded in the past two decades. Meert et al. (2021) provided an up-to-date assessment on Indian paleomagnetic data. A total of 11 poles were deemed high quality with R-values > 4 (Meert et al., 2020). Only two of the poles are available for the interval of Columbia tenure at 1765 Ma (Shankar et al., 2017; Pivarunas et al., 2021) and 1465 Ma (Pisarevsky et al., 2013). Due to the limited database, India's position within Columbia is not well known although the configuration proposed by Rogers and Santosh (2002,2009) is not supported (See Section 2.2). Zhao et al. (2002) link the 2.1–1.8 Ga Trans North China Orogen (TNCO) with the Central Indian Tectonic Zone (CITZ) and argued for proximity in the Columbia supercontinent. While both the CITZ and TNCO are important sutures within the two continents, the age of major orogenesis in the NCB and SIB are not coeval. The CITZ represents the suturing between the SIB/NIB around 1.1–1.0 Ga with a pulse of older ~ 1.6 Ga accretionary orogenic activity (Bhowmik, 2019) whereas the TNCO is a continent–continent collision between eastern and western blocks culminating between 1.95 and 1.8 Ga (Trap et al., 2012; Tang and Santosh, 2018). Meert (2012) referred to both the North China craton and India as 'lonely wanderers' because they were typically isolated along the margins of Columbia and Rodinia and their proposed links with other cratons was controversial. For example, India has been positioned near the North China Block sandwiched between Siberia and Northern Australia (Zhang et al., 2012); between Australia and Siberia (Chaves and de Rezende, 2019); between Baltica, Kalahari and Congo-São Francisco (Pisarevsky et al., 2014); along the margin of Columbia adjacent to Baltica (Elming et al., 2021); adjacent to Amazonia (Meert et al., 2021) and outboard of Columbia near the North China craton (Zhao et al., 2002; Xu et al., 2014; Shankar et al., 2017). While many of these reconstructions are paleomagnetically permissible, some of the proposed geological connections are incorrect (re: TNCO-CITZ). In addition, Pisarevsky et al. (2013) link the CITZ (1.6 Ga accretionary and 1.1–1.0 collisional) with the 2.1–1.9 Ga Lipetsk-Losev/East Voronezh Belt collisional belt between Volgo-Uralia and Sarmatia. The only reliable pole available from India during Columbia is derived from the 1.466 Ga Lakhna dykes (Pisarevsky et al., 2013). Elming et al. (2021) place India near Baltica during this interval; however, poles from Baltica indicate poor agreement with the proposed fit (Supplementary Table S-6). Better fits between the Laurentian, Siberian and North China poles with India were obtained in the ~ 1.49 Ga reconstruction.

There are no paleomagnetic poles for the Columbia supercontinent from the Congo craton; however, it is presumed that the Congo craton was attached to São Francisco since about 2.0 Ga (Akmim and Texeira, 2017). Two paleomagnetic poles from the Sao Francisco craton are dated to 1.794 Ga and 1.507 Ga. Elming et al. (2021) do not include the Amazonian-West African and Congo-Sao Francisco blocks in the Columbia supercontinent. Due to the limited data from the Congo-Sao Francisco craton, we do not consider them further.

4.5. Baltica-Laurentia in Columbia

Paleomagnetic data from Baltica and Laurentia are by far the most abundant and form the basis for a proposed long-lived connection in both Columbia and Rodinia. Comparison between Baltica-Laurentian poles in the Elming et al. (2021) reconstruction show that only 25% of the comparisons have E-values ≥ 0.2. The Elming et al. (2021) reconstruction follows the Nena proposal of Gower et al. (1990). In the 1.78 Ga "SAMBA" reconstruction ~ 62% of the Baltica-Laurentia poles have E-values ≥ 0.2 indicating a more reasonable match in a Nena-like configuration. Greenland is traditionally considered an integral part of Laurentia, and most reconstructions apply a Phanerozoic rotation to close the Labrador Sea (Roest and Srivastava, 1989). That fit does not bring Greenland poles into accordance with Laurentia suggesting alternative fits should be considered.

5. Conclusions

In this paper, we provide an updated synthesis of the Columbia supercontinent proposal. We also present a method for testing paleomagnetic reconstructions when data are unevenly spread in time and space. We provide examples of how that method was used to test the proposed SAMBA fit between Baltica, Amazonia and Laurentia and to test the Columbia model of Elming et al. (2021). While there are certain cases where the fits indicate a reasonable match to the proposals, most of the data show either poor fits or lead to ambiguous conclusions. Based on our analysis we conclude the following:

(1) Geological and geochronological data are consistent with the assembly and disaggregation of a large continental landmass in the Mesoproterozoic, but these data should also be supported by paleomagnetic data which requires a more robust statistical approach. Many reconstructions rely on a shotgun approach whereby data with slightly different ages and precision are lumped together and deemed 'close enough'.
(2) Our methodology provides an expanded error (C95) for each pair of poles which considers paleomagnetic errors along with age differences between poles. These expanded errors are then tested in a Bayesian framework (Heslop and Roberts, 2019) to assess goodness of fit.
(3) The Bayesian framework is based on a continuum in probability space. There is no set value at which a particular observation is deemed 'passing'; however, we argue that fits with Bayesian errors < 0.2 (after C95 adjustments) should be examined more closely.
(4) The proposed SAMBA connection between Baltica, Amazonia and Laurentia is an excellent example of the ambiguity in paleomagnetic data. Depending on the choice of pole for Amazonia at 1.78 Ga, the case can be made for a SAMBA-like connection between 1.78 and 1.5 Ga, but the fit is problematic at younger times.
(5) We tested the Columbia model of Elming et al. (2021) using the same procedure and found numerous discrepancies even after accounting for paleomagnetic errors and age differences.
(6) Our method can be applied to any reconstruction where data are unevenly distributed and provide a first-order statistical assessment of goodness of fit. A 'poor' fit may demand simple rotational adjustments to the proposed model or may indicate more severe problems (latitudinal misfits).
(7) Despite twenty years of progress, there is still a critical need for integrated paleomagnetic, geochronologic, and geologic data from all continents to fill in obvious gaps in the Columbia model. These data can only be generated by detailed field and laboratory work.

Declaration of Competing Interest

The authors declare that they have no known competing financial interests or personal relationships that could have appeared to influence the work reported in this paper.

Acknowledgements

The authors would like to thank Ms. Mia Luna and Mr. Owen Smith for their assistance with data compilation and analysis. We also thank Dr. Anthony Pivarunas and Dr. Scott Miller for their discussions regarding the techniques described in the paper. This work was supported by the US National Science Foundation grant EAR18-50693 to JGM. We thank editor Sanghoon Kwon for swift handling of the paper and Guochun Zhao and Zhiyu Yi for their comments on the original draft.

Appendix A. Supplementary material

Supplementary data to this article can be found online at https://doi.org/10.1016/j.gr.2022.06.014.

References

Abrahamsen, N., Van der Voo, R., 1987. Paleomagnetism of middle Proterozoic (c. 1.25 Ga) dykes from North Central Greenland. Geophys. J. Int. 91, 597–611.
Abrajevitch, A. and Van der Voo, R., 2010. Incompatible Ediacaran paleomagnetic directions suggest and equatorial geomagnetic dipole hypothesis, Earth Planet. Sci. Lett., 293-164-170.
Akmim, F.F., Texeira, W., 2017. The Paleoproterozoic Mineiro Belt and the Quadrilátero Ferrífero, in: Heilbron et al. (eds) The São Francisco craton and its margins, Eastern Brazil, Geology Review Series, Springer-Verlag Publishing, 71-94.
Almeida, M.E., Nascimiento, R.S.C., Mendes, T.A., Santos, J.O.S., Macembira, M.J.B., Vasconcelos, P., Pinheiro, S.S., 2021. An outline of Paleoproterozoic-Mesoproterozoic crustal evolution of the NW Amazon craton and implications for the Columbia supercontinent. Int. Geol. Rev. https://doi.org/10.1080/00206814.2021.2025155.
Bazhenov, M.L., Levahsova, N.M., Meert, J.G., 2016. How well do Precambrian paleomagnetic data agree with Phanerozoic apparent polar wander paths: A Baltica case study. Precambrian Res. 285, 80–90.
Bhowmik, S., 2019. The current status of orogenesis in the Central Indian Tectonic Zone: a view from the southern margin. Geol. J. 54, 2912–2934.
Bispos-Santos, F., D'Agrella-Filho, M.S., Pacca, I.I.G., Janikian, L., Trindade, R.I.F., Elming, S.Å., Barros, M.A.S., Pinho, F.E.C., 2008. Columbia revisited: paleomagnetic results from the 1790 Ma Colíder volcanics (SW Amazonian craton). Precambrian Res. 164, 40–49.
Bispos-Santos, F., D'Agrella-Filho, M.S., Trindade, R.I.F., Elming, S.Å., Jenikian, L., Vasconcelos, P.M., Parillo, B.M., Pacca, I.I.G., da Silva, J.A., Barros, M.A.S., 2012. Tectonic implications of the 1419 Ma Nova Guarita mafic intrusives paleomagnetic pole (Amazonian craton) on the longevity of Nuna. Precambrian Res. 196–197, 1–22.
Bispos-Santos, F., D'Agrella-Filho, M.S., Trindade, R.I.F., Jenikian, L., Reis, N., 2014. Was there a SAMBA connection in Columbia? Paleomagnetic evidence from the Avanavero mafic sills (northern Amazon craton). Precambrian Res. 244, 139–155.
Bispos-Santos, F., D'Agrella-Filho, M.S., Pesonen, L.J., Salminen, J.M., Reis, N.J., Silva, J. M., 2020. The long life of SAMBA connection in Columbia: A paleomagnetic study of the Mucajaí Complex, northern Amazonian craton. Gondwana Res. 80, 285–302.
Bogdanova, S.V., Bingen, B., Gorbatschev, R., Kheraskova, T.N., Kozlov, V.I., Puchkov, V.N., Volozh, Y.A., 2008. The East European craton (Baltica) before and after the assembly of Rodinia. Precambrian Res. 160, 23–45.
Boniface, N., Tsujimori, T., 2021. New tectonic model and division of the Ubendian-Usagaran belt, Tanzania: A review and in-situ dating of eclogites, doi:10.1130/2021.2552(8).
Bonin, B., 2007. A-type granites and related rocks: evolution of a concept, problems, and prospects. Lithos 97, 1–29.
Bono, R., Tarduno, J.A., Nimmo, F., Cottrell, R., 2019. Young inner core inferred from Ediacaran ultra-low geomagnetic field intensity. Nat. Geosci. 12. https://doi.org/10.1038/s41561-018-0288-0.
Cai, Y., Pei, J., Zhang, S-H., Tong, Y., Yang, Z., Zhao, Y., 2020. New paleomagnetic results from the ca 1.68-1.63 Ga mafic dye swarms in the western Shandong Province, eastern China: Implications for the reconstruction of the Columbia supercontinent, Precambrian Res., doi.1016/j.precamres.2019.105531.
Cawood, P.A., Tyler, I.M., 2004. Assembling and reactivating the Proterozoic Capricorn orogen: lithotectonic elements, orogenies and significance. Precambrian Res. 128, 201–218.
Cawood, P.A., Kroner, A., Collins, W.J., Kusky, T.M., Mooney, W.A., Windley, B.F., 2009. Accretionary orogens through Earth history. Geol. Soc. London Spec. Pub. 318, 1–36.
Charette, B., Godet, A., Guilmette, C., Davis, D.W., Vervoort, J., Kendall, B., Lafrance, I., Bandayera, D., Yakymchuk, C., 2021. Long-lived anatexis in the exhumed middle crust of the Torngat orogen: constraints from phase equilibria modelling and garnet, zircon and monazite geochronology. Lithos 388–389. 10.106/j.lithos.2021.1060222.
Chaves, A.D.O., de Rezende, C.R., 2019. Fragments of 1.79-1.75 Ga large igneous provinces in reconstructing Columbia (Nuna): A Statherian supercontinent-superplume coupling? Episodes 42, 55–67.
Chen, L., Huang, B., Yi, Z., Zhao, J., Yan, Y., 2013. Paleomagnetism of ca. 1.35 Ga sills in northern North China craton, ad implications for paleogeographic reconstruction of the Mesoproterozoic supercontinent. Precambrian Res. 228, 36–47.
Chiarenzelli, J., Aspler, L., Villeneuve, M., Lewry, J., 1998. Early Proterozoic evolution of the Saketchewan craton and its allochthonous cover, Trans-Hudson orogen. J. Geol. 106, 247–268.
Collins, A.J., 2003. Structure and age of the northern Leeuwin complex, western Australia: constraints from field mapping and U-Pb isotopic analysis. Aus. J. Earth Sci. 50, 589–599.
Collins, A.J., Pisarevsky, S., 2005. Amalgamating eastern Gondwana: The evolution of the circum-Indian orogenies, Earth Sci. Rev. 71, 229–270.
Condie, K.C., 2013. Preservation and recycling of crust during accretionary and collisional phases of Proterozoic orogens: a bumpy road from Nuna to Rodinia. Geosciences 3, 240–261.
Condie, K.C., Aster, R.C., 2010. Episodic zircon age spectra of orogenic granitoids: The supercontinent connection and continental growth: Precam. Res. 180, 227–236.
Condie, K.C., Arndt, N., Devaille, A., Puetz, S.J., 2017. Zircon age peaks: production or preservation of continental crust? Geosphere 13, 227–234.
Cordani, U.G., Sato, K., Sproenner, W., Fernandes, F.S., 2016. U-Pb zircon ages of rocks from the Amazonas territory of Colombia and their bearing on the tectonic history of the NW sector of the Amazonian craton. Braz. J. Geol. 46, 5–35.
D'Agrella-Filho, M.S., Trindade, R.I.F., Elming, S.-Å., Texeira, W., Yokoyama, E., Tohver, E., Geraldes, M.C., Pacca, I.I.G., Barros, M.A.S., Ruiz, A.S., Tohver, E., Ruiz, A.S., 2012. The 1420 Ma Indiavaí mafic intrusion (SW Amazonian craton): Paleomagnetic results and implications for the Columbia supercontinent. Gondwana Res. 22, 956–973.
D'Agrella-Filho, M.S., Trindade, R.I.F., Queiroz, M.V.B., Meira, M.T., Janikian, L., Ruiz, A.S., 2016. Reassessment of Aguapei (Salto de Céu) paleomagnetic pole of the Amazonian craton and implications for Proterozoic supercontinents. Precambrian Res. 272, 1–17.
D'Agrella-Filho, M.S., Antonio, P.Y.J., Trindade, R.I.F., Texeira, W., Bispos-Santos, F., 2021. Chapter 6: The Precambrian drift history and paleogeography of Amazonia, in: Pesonen et al. (eds) Ancient Supercontinents and the Palaeogeography of the Earth, ISBN:978-0-12-818533-9, pp. 207-241.
Darbyshire, F.A., Bartow, I.D., Petrescu, L., Gilligan, A., 2017. A tale of two orogens: Crustal processes in the Proterozoic Trans-Hudson and Grenville orogens, eastern Canada. Tectonics 36, 1633–1659.
Davis, W.J., Sanborn-Barrie, M., Berman, R.G., Pehrsson, S., 2021. Timing and provenance of Paleoproterozoic supercrustal rocks in the central Thelon tectonic zone, Canada: implications for the tectonic evolution of western Laurentia from ca. 2.1 to 1.9 Ga. Can. J. Earth Sci. 58, 378–395.
Donskaya, T.V., 2020. Assembly of the Siberia craton: constraints from Paleoproterozoic granitoids. Precambrian Res. 348. https://doi.org/10.1016/2020.105869.
Elming, S.-Å., 1985. A paleomagnetic study of Svecokarelian basic rocks from northern Sweden. Geol. Fören. Stockholm Förhan. 107, 17–35.
Elming, S.-Å., 1994. Palaeomagnetism of Precambrian rocks in northern Sweden and its correlation to radiometric data. Precambrian Res. 69, 61–79.
Elming, S.-Å., Moakhar, M.O., Layer, P., Donadini, F., 2009. Uplift deduced from remanent magnetization of a Proterozoic basic dyke and the baked country rock in the Hoting area, central Sweden: a palaeomagnetic and $^{40}Ar/^{39}Ar$ study. Geophys. J. Int. 179, 59–78.
Elming, S-Å., Salminen, J., Pesonen, L., 2021. Chapter 16. Paleo-Mesoproterozoic Nuna Supercycle, in: Pesonen et al. (eds) Ancient Supercontinents and the Palaeogeography of the Earth, ISBN:978-0-12-818533-9, pp. 499-548.
Elston, D.P., Enkin, R.J., Baker, J., Kisilevsky, D.K., 2002. Tightening the Belt: paleomagnetic-stratigraphic constraints on deposition, correlation and deformation of the Middle Proterozoic (ca. 1.4 Ga) Belt-Purcell Supergroup. United States and Canada. Bull. Geol. Soc. Am. 114, 619–638.
Emslie, R.F., Irving, E., Park, J.K., 1976. Further paleomagnetic results from the Michikamau intrusion, Labrador. Can. J. Earth Sci. 13, 1052–1057.
Ernst, R.E., Buchan, K.L., Hamilton, M.A., Okrugin, A., Tomshin, M.D., 2000. Integrated paleomagnetism and U-Pb geochronology of mafic dykes of the Eastern Anabar Shield Region, Siberia: Implications for Mesoproterozoic paleolatitude of Siberia and comparison with Laurentia. J. Geol. 108, 381–401.
Ernst, R.E., Wingate, M.T.D., Buchan, K.L., 2008. Global record of 1600–700 Ma Large Igneous Provinces (LIPs): implications for the reconstruction of the proposed Nuna (Columbia) and Rodinia supercontinents. Precambrian Res. 160, 159–178.
Ernst, R.E., Hamilton, M.A., Söderlund, U., Hanes, J.A., Gladkochub, D.P., Okrugin, A. V., Kolutilina, T., Makhonoshin, A.S., Bleeker, W., LeChaminant, A.N., Buchan, K. L., Chamberlain, D., A.n.,, 2016. Long-lived connection between Siberia and northern Laurentia in the Proterozoic. Nat. Geosci. 9, 464–469.
Evans, D.A.D., 2006. Proterozoic low orbital obliquity and axial-dipolar geomagnetic field from evaporite paleolatitudes. Nature 444, 51–55.
Evans, D.A.D., Mitchell, R.N., 2011. Assembly and breakup of the core of Paleoproterozoic-Mesoproterozoic supercontinent Nuna. Geology 39, 443–446.
Evans, D.A.D., Veselovsky, R.V., Petrov, P.Y., Shatsillo, A.V., Pavlov, V.E., 2016. Paleomagnetism of Mesoproterozoic margins of the Anabar Shield: A hypothesized billion-year partnership of Siberia and northern Laurentia. Precam. Res. 281, 639–655.

Evans, D.A.D., Pesonen, L.J., Eglington, B.M., Elming, S-Å, Gong, Z., Li, Z-X., McCausland, P.J., Meert, J.G., Mertanen, S., Pisarevsky, S.A., Pivarunas, A.F., Salminen, J., Swanson-Hysell, N.L., Torsvik, T.H., Trindade, R.I.F., Veikkolainen, T., Zhang, S., 2021. Chapter 19: An expanding list of reliable paleomagnetic poles for Precambrian tectonic reconstructions, in: Pesonen et al. (eds) Ancient Supercontinents and the Palaeogeography of the Earth, ISBN:978-0-12-818533-9, pp. 605-639.

Fahrig, W.F., Jones, D.L., 1976. The paleomagnetism of the Helikian Mistatin pluton, Labrador, Canada. Can. J. Earth Sci. 13, 832–837.

Fedotova, M.A., Khramov, A.N., Pisakin, B.N., Priyatkin, A.A., 1999. Early Proterozoic paleomagnetism: new results from the intrusive and related rocks of the Karelian, Belomorian and Kola provinces, eastern Fennoscandian Shield. Geophys. J. Int. 137, 691–712.

Fisher, R., 1953. Dispersion on a sphere. Proc. R. Soc. Lond. A217, 295–305.

Frost, C.D., Frost, B.R., 2011. On Ferroan (A-type) granitoids: their compositional variability and modes of origin. J. Petrol. 52, 39–53.

Gala, M.G., Symons, D.T.A., Palmer, H.C., 1995. Paleomagnetism of the Jan Lake Granite, Trans-Hudson Lake Orogen. Saskatchewan. Geol. Surv. Misc. Rep. 95, 145–152.

Gladkochub, D.P., Donskaya, T.V., Mazubkabzov, A.M., Stanevich, A.M., Sklyarov, E. V., Ponomaarchuk, V.A., 2007. Signature of Precambrian extension events in the southern Siberian craton. Russ. Geol. Geophys. 48, 17–31.

Godet, A., Guilmette, C., Labrosse, L., Smit, M.A., Davis, D.W., Ramondo, T., Vanier, M.-A., Charette, B., Lafrance, I., 2020. Contrasting P-T-t paths reveal a metamorphic discontinuity in the New Quebec orogen: insights into Paleoproterozoic orogenic processes. Precambrian Res. 342. https://doi.org/10.1016/j.precamres.2020.105675.

Gordon, R., Cox, A., 1980. Calculating paleomagnetic poles for oceanic plates. Geophys. J. Int. 63, 619–640.

Gower, C.F., Ryan, A.B., Rivers, T., 1990. Mid-Proterozoic Laurentia-Baltica; an overview of its geological evolution and a summary of the contributions made by this volume, in Gower et al. (eds): Mid-Proterozoic Laurentia-Baltica, Geol. Assoc. Canada Spec. Paper 38, 1-20.

Gray, D.R., Foster, D.A., Meert, J.G., Goscombe, B.D., Armstrong, R., Truow, R.A.J., Passchier, C.W., 2008. A Damaran perspective on the assembly of southwestern Gondwana. Geol. Soc. Lon. Spec. Pub. 294, 257–278.

Grenholm, M., 2019. The global context of the 2.27-1.96 Birimian orogeny-insights from comparative studies, with implications for supercontinental cycles. Earth Sci. Rev. 193, 260–298.

Halls, H.C., Hamilton, M.A., Denyszyn, S.W., 2011. The Melville dyke swarm of Greenland: A connection to the 1.5-1.6 Ga Fennoscandian rapakivi granite province, in: Srivastava, R.K. (ed) Dyke Swarms: Keys for Geodynamic Interpretation, Springer-Verlag, Berlin, Germany, pp. 509-536.

Harlan, S., Geissman, J.W., 1998. Paleomagnetism of the Middle Proterozoic Electra Lake Gabbro, Needle Mountains, southwestern Colorado. J. Geophys. Res. 103, 15497–15507.

Harlan, S., Snee, L.W., Geissman, J.W., Brearley, A.J., 1994. Paleomagnetism of the Middle Proterozoic Laramie anorthosite complex and Sherman Granites, southern Laramie range, Wyoming and Colorado. J. Geophys. Res. 99 (17997–18), 020.

Hawkesworth, C., Cawood, P., Dhuime, B., 2013. Continental growth and the crustal record: Tectonophysics 609, 651–660.

Heslop, D., Roberts, A., 2019. Quantifying the similarity of paleomagnetic poles. J. Geophys. Res. 124. https://doi.org/10.1029/2019JB018342.

Hildebrand, R.S., Hoffman, P.F., Bowring, S.A., 2010. The Calderian orogeny in the Wopmay Orogen (1.9 Ga) northwestern Canadian shield. Bull. Geol. Soc. Am. 122, 794–814.

Hinchey, A.M., 2021. Lithogeochemical and Nd isotopic constraints on felsic magmatism in the Makkovik orogen, Labrador, Canada: implications for assembly of the supercontinent Nuna, Lithos, 382-383, j.lithos.2020.105917.

Hoffman, P.F., 1997. Tectonic genealogy of North America. In: van der Pluijm, B.A., Marshak, S. (Eds.), Earth Structure: An Introduction to Structural Geology and Tectonics. McGraw-Hill, New York, pp. 459–464.

Huakin, L., Wenbo, S., Hongying, Z., Zhengun, X., Hui, T., Ligong, Y., Huff, W., Ettensohn, F., 2014. The first precise age constraints on the Jixian System of the Meso-to Neoproterozoic standard section of China: SHRIMP zircon U-Pb dating of bentonites from the Wumishan and Tieling Formations in the Jixian section, North China craton. Acta Pet. Sin., 2999–3012

Idnurm, M., 2000. Toward a high-resolution Late Palaeoproterozoic-Early Mesoproterozoic apparent polar wander path for northern Australia. Aus. J. Earth Sci. 47, 405–429.

Idnurm, M., Giddings, J.W., Plumb, K.A., 1995. Apparent polar wander path and reversal stratigraphy of the Palaeoproterozoic-Mesoproterozoic southeastern MacArthur Basin. Australia, Precambrian Res. 72, 1–41.

Irving, E., Donaldson, J., Park, J.K., 1972. Paleomagnetism of the Western Channel diabase and associated rocks. Northwest Territories. Can. J. Earth Sci. 9, 960–971.

Irving, E., Baker, J., Hamilton, M., Wynne, P.J., 2004. Early Paleoproterozoic geomagnetic field in western Laurentia: implications for paleolatitudes, local rotations and stratigraphy. Precambrian Res. 129, 251–270.

Johannson, A., 2009. Baltica and Amazonia and the SAMBA connection-1000 million years of neighbourhood during the Proterozoic? Precambrian Res. 175, 221–234.

Johannson, A., Bingen, B., Huhma, H., Waight, T., Vestergaard, R., Soesoo, A., Skridlaite, G., Krzeminsko, E., Shumlyansky, L., Holland, M.E., Holm-Danoma, C., Texeira, W., Faleros, F.M., Ribeiro, B.V., Jacobs, J., Wang, C., Thomas, R.J., Macey, P.H., Kikland, C.L., Hartnady, M.I.H., Eglington, B.M., Puetz, S.J., 2022. A geochronological review of magmatism along the external margin of Columbia and in Grenville-age orogens forming the core of Rodinia. Precambrian Res. https://doi.org/10.1016/j.precamres.2021.106463.

Johnson, S.P., Thorne, A.M., Tyler, M., Korsch, R.J., Kennett, B.L.N., Cutten, H.N., Aitken, A.R.A., Holzschuh, J., Salmon, M., Reading, A., Heinson, G., Boren, G., Ross, J., Costelloe, R.D., Fomin, T., 2013. Crustal architecture of the Capricorn Orogen, western Australia, and associate metallogeny. Aus. J. Earth Sci. 60, 681–705.

Karlstrom, K.E., Harlan, S.S., Williams, M.L., McClelland, J., Geissman, J.W., Ahäll, K.-I., 1999. Refining Rodinia: Geologic evidence for the Australia-western US connection in the Proterozoic. GSA Today 9, 2–6.

Kent, D.V., Smethurst, M.A., 1998. Shallow bias of paleomagnetic inclinations in the Paleozoic and Precambrian. Earth Planet. Sci. Lett. 160, 391–402.

Killian, T.M., Chamberlain, K.R., Evans, D.A.D., Bleeker, W., Cousens, B.L., 2016. Wyoming on the run-toward the final Paleoproterozoic assembly of Laurentia. Geology 44, 863–866.

Kirscher, U., Nordsvan, A., Schmidt, P., 2021a. Whence Australia? Its Precambrian drift history and paleogeography, in: Pesonen et al. (eds) Ancient Supercontinents and the Palaeogeography of the Earth, ISBN:978-0-12-818533-9, pp. 277-306.

Kirscher, U., Mitchell, R.N., Liu, Y., Nordsvan, A.R., Cox, G.M., Pisarevsky, S.A., Wang, C., Wu, L., Murphy, J.B., Li, Z.-X., 2021b. Paleomagnetic constraints on the duration of the Australia-Laurentia connection in the core of the Nuna supercontinent. Geology 49, 174–179.

Kolb, J., 2014. Structure of the Paleoproterozoic Nagssugtoqidian Orogen, South-East Greenland: model foe the tectonic evolution. Precambrian Res. 255, 809–822.

Korja, A., Heikkinen, P., 2005. The accretionary Svecofennian orogen-insight from the BABEL profiles. Precambrian Res. 136, 241–268.

Korja, A., Heikkinen, P., 2008. Seismic images of Paleoproterozoic microplate boundaries in the Fennoscandian shield. Geol. Soc. Am. Spec. Pap. 440. https://doi.org/10.1130/2008.2440(11).

Korja, A., Lahtinen, R., Niroven, M., 2006. The Svecofennian orogen: A collage of microcontinents and island arcs. Geol. Soc. London Mem. 32, 561–578.

Kulakov, E.V., Slagstad, T., Ganerød, M., Torsvik, T.H., 2022. Paleomagnetism and $^{40}Ar/^{39}Ar$ geochronology of Meso-Neoproterozoic rocks from southwest Norway. Implications for magnetic remanence ages and the paleogeography of Baltica in a Rodinia supercontinent context, Precambrian Res., in press.

Lubnina, N.V., 2009. The East European craton in the Mesoproterozoic: New key paleomagnetic poles. Dokl, Earth Sci. 428, 1174–1178.

Lubnina, N., Mertanen, S., Söderlund, U., Bogdanova, S., Vasilieva, T.I., 2010. A new key paleomagnetic pole for the East European craton at 1452 Ma: paleomagnetic and geochronological constraints from mafic rocks in the Lake Ladoga region (Russian Karelia). Precambrian Res. 183, 442–462.

Lubnina, N.V., Pisarevsky, S.A., Söderlund, U., Nilsson, M., Sokolov, S.J., Khramov, A. N., 2012. New palaeomagnetic and geochronological data from the Ropruchey sill (Karelia Russia): implications for late Palaeoproterozoic palaeogeography. In: Mertanen, S., Pesonen, L.J., Sangchan, P. (Eds.). Supercontinent symposium 2012—Programme and Abstracts. Geological Survey of Finland, Espoo, Finland, pp. 81_82.

Luoto, T., Salminen, J., Obst, K., 2021. Revisting mafic dykes of Bornholm-implications for Baltica in supercontinent Nuna and 1.3 Ga. Precambrian Res. 367. https://doi.org/10.1016/j.precamres.2021.106444.

Marcussen, C., Abrahamsen, N., 1983. Paleomagnetism of the Midsommersø dolerites, eastern North Greenland. Geophys. J.R. astr Soc. 73, 367–387.

Markwitz, V., Kirkland, C.L., Evans, N.J., 2017. Early Cambrian metamorphic zircon in the northern Pinjarra orogen: implications for the structure of the west Australian cratonic margin. Lithosphere 9, 3–13.

McFadden, P.L., Lowes, F.J., 1981. The discrimination of mean directions drawn from Fisher distributions. Geophys. J. Roy. Astr. Soc. 67, 19–33.

McFadden, P.L., McElhinny, M.W., 1990. Classification of the reversal test in palaeomagnetism. Geophys. J. Int. 103, 725–729.

Metelkin, D.V., Belonosov, I.V., Gladkochub, D.P., Donskaya, T.V., Mazukabzov, A.M., Stanevich, A.M., 2005. Paleomagnetic directions from Nersa intrusions of the Biryusa Terrane, Siberian Craton, as a reflection of tectonic events in the Neoproterozoic. Russ. Geol. Geophys. 46, 398–413.

Meert, J.G., 2002. Paleomagnetic evidence for a Paleo-Mesoproterozoic supercontinent Columbia. Gondwana Res. 5, 207–215.

Meert, J.G., 2003. A synopsis of events related to the assembly of eastern Gondwana. Tectonophysics 362, 1–40.

Meert, J.G., 2009. News and Views. In GAD we trust, Nature Geosc. 2, 673–674.

Meert, J.G., 2012. What's in a name? The Columbia (Palaeopangea/Nuna) Supercontinent. Gondwana Res. 21, 987–993.

Meert, J.G., 2014. Strange Attractors, Spiritual Interlopers and Lonely Wanderers: The Search for Pre-Pangæan Supercontinents. Geosci. Front. 5, 155–166.

Meert, J.G., Stuckey, W., 2002. Revisiting the paleomagnetism of the 1.476 Ga St. Francois Mountains igneous province, Missouri. Tectonics 21. https://doi.org/10.1029/2000TC001265.

Meert, J.G., Lieberman, B.S., 2008. The Neoproterozoic assembly of Gondwana and its relationship to the Ediacaran-Cambrian Radiation. Gondwana Res. 14, 5–21.

Meert, J.G., Torsvik, T.H., 2003. The making and unmaking of a supercontinent: Rodinia Revisited. Tectonophysics 375, 261–288.
Meert, J.G., Santosh, M., 2017. The Columbia supercontinent revisited. Gondwana Res. 50, 67–83.
Meert, J.G., Van der Voo, R., Ayub, S., 1995. Paleomagnetic investigation of the Neoproterozoic Gagwe lavas and Mbozi Complex, Tanzania and the assembly of Gondwana. Precam. Res. 74, 225–244.
Meert, J.G., Tamrat, E., Spearman, J., 2003. Non-dipole fields and inclination bias: insights from a random walk analysis. Earth Planet. Sci. Lett., 395–408
Meert, J.G., Pivarunas, A.F., Miller, S.R., Evans, D.A.D., Pisarevsky, S., Pesonen, L., Elming, S.A., Li, Z.X., Zhang, S., 2020. Paleomagnetic Reliability: The Van der Voo (1990) Quality Scale Revisited. Tectonophys. https://doi.org/10.1016/tecto.2020.228549.
Meert, J.G., Pivarunas, A.F., Miller, S.R., Pandit, M.K., Sinha, A.K., 2021. Chapter 10. The Precambrian drift history and paleogeography of India, in: Pesonen et al. (eds) Ancient Supercontinents and the Palaeogeography of the Earth, ISBN:978-0-12-818533-9, pp. 305-327.
Mertanen, S., Pesonen, L.J., 1995. Paleomagnetic and rock magnetic investigations of the Sipoo quartz porphyry and diabase dykes, southern Fennoscandia. Phys. Earth Planet. Int. 88, 145–175.
Mertanen, S., Eklund, O., Shebanov, A., Frank-Kamenetsky, D., 2006. Paleo- and Mesoproterozoic dyke swarms at Lake Ladoga area, NW Russia—paleomagnetic studies. In: Hanski, E., Mertanen, S., Ramo, T., Vuollo, J. (Eds.), Dyke Swarms—Time Markers of Crustal Evolution, Geological. Taylor & Francis, London, pp. 63–74.
Mitchell, R.N., Zhang, N., Salminen, J., Liu, Y., Spencer, C.J., Steinberger, B., Murphy, J. B., Li, Z.-X., 2021. The supercontinent cycle. Nature Rev. Earth Environ. 2, 358–374.
Moakhar, M.O., 1998. Rapakivi granite and basic dykes in the Fennoscandian shield: A paleomagnetic analysis (Ph.D. thesis). Luleå University, p. 40 pp..
Moores, E.M., 1991. Southwest U.S.-East Antarctica (SWEAT) connection: A hypothesis. Geology 19, 425–428.
Morrisey, L.J., Barovich, K.M., Hand, M., Howard, K.E., Payne, J.L., 2019. Magmatism and metamorphism at ca. 1.45 Ga in the northern Gawler craton,: The Australia record of rifting within Nuna (Columbia). Geosci. Front. 10, 175–194.
Murthy, G.S., 1978. Paleomagnetic results from the Nain anorthosite and their tectonic implications. Can. J. Earth Sci. 15, 516–525.
Murthy, G.S., Fahrig, W.F., Jones, D.L., 1968. The paleomagnetism of the Michikamau anorthositic intrusion. Labrador. Can. J. Earth Sci. 5, 1139–1144.
Neuvonen, K.J., 1986. On the direction of remanent magnetization of the quartz porphyry dikes in SE Finland. Geol. Surv. Finland Bull. 53, 109–133.
Neves, S.P., 2021. Comparative geological evolution of the Borborema Province and São Francisco craton (eastern Brazil): Decratonization and crustal reworking during West Gondwana assembly and implications for paleogeographic reconstructions. Precambrian Res. 49. https://doi.org/10.1016/j.precamres.2021.106119.
Nordsvan, A.R., Collins, W.J., Li, Z.-X., Spencer, C.J., Pourteau, A., Withnall, I.W., Betts, P.G., Volante, S., 2018. Laurentian crust in northeast Australia: implications for the assembly of the supercontinent Nuna. Geology 46, 251–254.
Palencia-Ortas, A., Ruiz-Martínez, V.C., Villalaín, J.J., Osete, M.L., Vegas, R., Touil, A., Hafid, A., McIntosh, G., van Hinsbergen, D.J.J., Torsvik, T.H., 2011. A new 200 Ma paleomagnetic pole forAfrica, and paleo-secular variation scatter from Central Atlantic Magmatic Province (CAMP) intrusives in Morocco (Ighrem and FoumZguid dykes). Geophys. J. Int. 185, 1220–1234.
Panzik, J.E., Evans, D.A.D., 2014. Assessing the GAD hypothesis with paleomagnetic data from large Proterozoic dike swarms. Earth Planet Sci. Lett. 406, 134–141.
Park, J.K., Irving, E., Donaldson, J.A., 1973. Paleomagnetism of the Precambrian Dubawnt Group. Bull. Geol. Soc. Am. 84, 859–870.
Payne, J.L., Hand, M., Barovich, K., Reid, A., Evans, D.A.D., 2009. Correlations and reconstruction models for the 2500–1500 Ma evolution of the Mawson continent. Geol. Soc. London Spec. Pub 323, 319–355.
Pehrsson, S.J., Eglington, B.M., Evans, D.A.D., Huston, D., Reddy, S.M., 2015. Mettalogeny and its link to orogenic style during the Nuna supercontinent. Geol. Soc. London Spec. Pub. 424, 83–94.
Pei, J., Yang, Z., Zhao, Y., 2006. A Mesoproterozoic paleomagnetic pole from the Yangzhuang formation, North China and its tectonic implications. Precambrian Res. 151, 1–13.
Pesonen, L.J., Mertanen, S., Veikkolainen, T., 2012. Paleo-Mesoproterozoic supercontinents-a paleomagnetic view. Geophysica 48, 5–47.
Piper, J.D.A., 1979. A paleomagnetic survey of Jotnian dolerites of central East Sweden. Geophys. J. Roy. Astr. Soc. 56, 451–479.
Piper, J.D.A., Grant, S., 1989. A palaeomagnetic test of the axial dipole assumption and implications for continental distribution through geological time. Phys. Earth Planet. Inter. 55, 37–53.
Pisarevsky, S., Bylund, G., 2010. Palaeomagnetism of the 1780–1770 Ma mafic and composite intrusions of Småland (Sweden): implications for the Mesoproterozoic supercontinent. Am. J. Sci. 310, 1168–1186.
Pisarevsky, S.A., Sokolov, S.J., 2001. The magnetostratigraphy and a 1780 Ma palaeomagnetic pole from the red sandstones of the Vazhinka River section, Karelia, Russia. Geophys. J. Int. 146, 531–538.
Pisarevsky, S.A., Biswal, T.K., Wang, X.-C., de Waele, B., Ernst, R., Soderlund, U., Tait, J. A., Ratre, K., Singh, Y.K., Cleve, M., 2013. Paleomagnetic, geochronological and geochemical study of Mesoproterozoic Lakhna dykes in the Bastar craton, India: Implications for the Mesoproterozoic supercontinent. Lithos 174, 125–143.
Pisarevsky, S.A., Elming, S.-Å., Pesonen, L.J., Li, Z.-X., 2014. Mesoproterozoic paleogeography: Supercontinent and beyond: Precam. Res. 244, 207–225.
Pisarevsky, S.A., Gladkochub, D.P., Donskaia, T.V., 2021. Chapter 8. Precambrian paleogeography of Siberia, in: Pesonen et al. (eds) Ancient Supercontinents and the Palaeogeography of the Earth, ISBN:978-0-12-818533-9, pp. 263-276.
Pivarunas, A.F., Meert, J.G., 2020. Intracratonic stability: A comparison of paleomagnetic data from north and south of the Dharawar craton. Precam. Res. 348. https://doi.org/10.1016/j.precamres.2020.105858.
Pivarunas, A.F., Meert, J.G., Katusin, K., Miller, S., Pandit, M.K., Craver, A., Roderus, K., Sinha, A.K., 2021. Paleomagnetic results from the Singhbhum craton, India: Demagnetization, remagnetization and complication, Precam. Res., doi.10.1016/j.precamres.2021.106165.
Pourteau, A., Smit, M.A., Li, Z.-X., Collins, W.J., Nordsvan, A.R., Volante, S., Li, J., 2018. 1.6 Ga crustal thickening along the final Nuna suture. Geology 46, 959–962.
Reis, N.J., Texeira, W., Hamilton, M.A., Bispos-Santos, F., Almeida, M.E., D'Agrella-Filho, M.S., 2013. Avanavero mafic magmatism, a late Paleoproterozoic LIP in the Guiana Shield, Amazonian craton. Lithos 174, 175–195.
Roberts, N.M.W., Slagstad, T., 2014. Continental growth and reworking on the edge of Columbia and Rodinia supercontinents; 1.86-0.9 Ga accretionary orogeny in SW Fennoscandia. Int. Geol. Rev. 57. https://doi.org/10.1080/002068414.2014.958579.
Roest, W.R., Srivastava, S.P., 1989. Sea-floor spreading in the Labrador Sea: A new reconstruction. Geology 17, 1000–1003.
Rogers, J.J.W., 1993. India and Ur. J. Geol. Soc. India 42, 217–222.
Rogers, J.J.W., 1996. A history of continents in the past three billion years. J. Geology 104, 91–107.
Rogers, J.J.W., 2003. John Rogers: An autobiographical sketch. Gondwana Res. 6, 353–356.
Rogers, J.J.W., Santosh, M., 2002. Configuration of Columbia, a Mesoproterozoic supercontinent. Gondwana Res. 5, 5–22.
Rogers, J.J.W., Santosh, M., 2004. Continents and Supercontinents. Oxford University Press, Oxford, p. 289.
Rogers, J.J.W., Santosh, M., 2009. Tectonics and surface effects of the supercontinent Columbia. Gondwana Res. 15, 373–380.
Rowley, D.B., 2019. Comparing paleomagnetic study mean with apparent polar wander paths: A case study and paleomagnetic test of the Greater India versus Greater Indian Basin hypothesis. Tectonics 38, 722–740.
Salminen, J., Pesonen, L.J., 2007. Paleomagnetic and rock magnetic study of the Mesoproterozoic sill. Valaam Island, Russian Karelia, Precambrian Res. 154, 212–230.
Salminen, J., Mertanen, S., Evans, D.A.D., Wang, Z., 2014. Paleomagnetic and geochemical studies of the Mesoproterozoi Satakunta dyke swarms, Finland, with implications for a Northern Europe-North America (NENA) connection within Nuna supercontinent. Precambrian Res. 244, 170–191.
Salminen, J., Klein, R., Mertanen, S., Pesonen, L.J., Fröjdö, S., Irmeli, M., Eklund, O., 2015. Paleomagnetism and U-Pb geochronology of ca. 1570 intrusives from Åland archipelago SW Finland-implications for Nuna. Geol. Soc. London Spec. Pub. 424, 95–118.
Salminen, J.M., Evans, D.A.D., Trindade, R.I.F., Oliveira, E.P., Piispa, E.J., Smirnov, A.V., 2016. Paleogeography of the Congo-São Francsisco craton at 1.5 Ga: expanding the core of the Nuna supercontinent. Precambrian Res. 286, 195–212.
Salminen, J., Klein, R., Veikkolainen, T., Mertanen, S., Mäntäri, I., 2017. Mesoproterozoic geomagnetic reversal asymmetry in light of new paleomagnetic and geochronological data from the Häme dyke swarm, Finland: Implications for the Nuna supercontinent. Precambrian Res. 288, 1–22.
Salminen, J., Klein, R., Mertanen, S., 2019. New rock magnetic and paleomagnetic results from the 1.64 Ga Suomenniemi dyke swarm. SE Finland, Precambrian Res. 329, 195–210.
Sears, J.W., 2022. Challenging the dipolar paradigm for Proterozoic Earth. Geol. Soc. Am. Spec. Pap. 553. https://doi.org/10.1130/2021.2553(17).
Sears, J.W., Price, R.A., 1978. The Siberian connection: A case for the Precambrian separation of the North American and Siberian cratons. Geology 6, 267–270.
Sears, J.W., Price, R.A., 2003. Tightening the Siberian connection to western Laurentia. Geol. Soc. Am. Bull. 115, 943–953.
Shankar, R., Sarma, D.S., Babu, N.R., Parashuramulu, V., 2017. Paleomagnetic study of 1765 Ma dyke swarm from the Singhbhum craton: Implications to the paleogeography of India. J. Asian Earth Sci. 157, 235–244.
Sklyarov, E.V., Gladkochub, D.P., Mazukabzov, A.M., Menshagin, Y.V., Watanabe, T., Pisarevsky, S.A., 2003. Neoproterozoic mafic dike swarms of the Sharyzhalgai metamorphic massif (southern Siberian craton). Precambrian Res. 122, 359–376.
Stern, R.J., 1994. Arc assembly and continental collision in the Neoproterozoic East Africa orogen: implications for the consolidation of Gondwanaland. Ann. Rev. Earth Planet. Sci. 22, 319–351.
Stern, R.J., 2018. The evolution of plate tectonics. Phil. Trans. Roy. Soc. A 376. https://doi.org/10.1098/2017.0406.
Swanson-Hysell, N.L., Maloof, A.C., Weiss, B.P., Evans, D.A.D., 2009. No asymmetry in geomagnetic reversals recorded by 1.1-billion-year-old Keweenawan basalts. Nat. Geosci. 2, 713–717.
Swanson-Hysell, N.L., Avery, M., Zhang, Y., Hodgin, E.B., Sherwood, R.J., Apen, F.E., Boerboom, T.J., Keller, C.B., Cottle, J.M., 2021. The paleogeography of Laurentia in its early years: New constraints from the Paleoproterozoic East-Central Minnesota batholith. Tectonics 40. https://doi.org/10.1029/2021.TC006751.
Tang, L., Santosh, M., 2018. Neoarchean-Paleoproterozoic terrane assembly and Wilson cycle in the North China craton: an overview from the central segment of the Trans-North China Orogen. Earth Sci Rev. 182, 1–27.
Terentiev, R.A., Santosh, M., 2020. Baltica (East European craton) and Altantica (Amazonia and West African cratons in the Proterozoic: The pre-Columbia

connection. Earth Sci. Rev. 210. https://doi.org/10.1016/j.earthscirev.2020.103378.
Thallner, D., Biggin, A.J., McCausland, P.J.A., Fu, R.R., 2021a. New paleointensities from the Skinner Cove Formation, Newfoundland, suggesting a changing state of the geomagnetic field at the Ediacaran-Cambrian transition. J. Geophys. Res. 126. https://doi.org/10.1029/2021JB022292.
Thallner, D., Biggin, A.J., Halls, H.C., 2021b. An extended period of extremely weak geomagnetic field suggested by paleointensities from Ediacaran Grenville dykes (SE Canada). Earth Planet. Sci. Lett. 568. https://doi.org/10.1016/j.epsl.2021.1176025.
Thallner, D., Scherbakova, V.V., Bakhmutov, V.G., Scherbakov, V.P., Zhidkov, G.V., Polachencko, I.B., Biggin, A.J., 2022. New paleodirections and paleointensity data from extensive profiles through the Ediacaran section of the Volhyn Basalt Province (NW Ukraine). Geophys. J. Int. https://doi.org/10.1093/gji/ggac186.
Torsvik, T.H., Van der Voo, R., Preeden, U., MacNiocaill, C., Steinberger, B., Doubrovine, P.V., van Hinsbergen, D.J.J., Domev, M., Gaina, C., Tohver, E., Meert, J.G., McCausland, P.J.A., Cocks, L.R.M., 2012. Phanerozoic polar wander, paleogeography and dynamics. Earth Sci Rev. 114, 325–368.
Trap, P., Faure, M., Lin, W., Le Breton, N., Moiné, P., 2012. Paleoproterozoic tectonic evolution of the Trans-North China Orogen: toward a comprehensive model. Precambrian Res. 222–223, 191–211.
Vaes, B., Gallo, L.C., van Hinsbergen, D.J.J., 2022. On pole position: causes of dispersion of the paleomagnetic poles behind apparent polar wander paths, J. Geophys. Res., doi:10.1029/2022JB023953.
Vasquez, M.L., Cordani, U.G., Sato, K., Barbosa, J.P.O., Franco, M.T.L., Maurer, V.C., 2019. U-Pb SHRIMP dating of basement rocks of the Irori-Xingo domain, Central Amazonian Province, Amazonian craton, Brazil. Braz. J. Geol. 49. https://doi.org/10.1590/2317-4889201920190067.
Vasyukova, E.A., Metelkin, D.V., Letnikov, F.A., Letnikova, E.F., 2019. New isotope constraints on the time of formation of the Nersa dolerite complex from Biryusa-Sayan area. Dokl. Earth Sci. 485, 363–367.
Veikkolainen, T., Pesonen, L.J., 2021. Precambrian geomagnetic field-an overview. in: Pesonen et al. (eds) Ancient Supercontinents and the Palaeogeography of the Earth, ISBN:978-0-12-818533-9, pp. 81-108.
Vermeesch, P., 2018. IsoplotR: A free and open toolbox for geochronology. Geosci. Front. 9, 1479–1493.
Veselovskiy, R.V., Pavlov, V.E., Petrov, P.Y., 2009. New paleomagnetic data on the Anabar Uplift and Uchur-Maya region and their implications for the paleogeography and geological correlation of the Riphean of the Siberian Platform. Izvest. Phys. Solid Earth 45, 545–566.
Volante, S., Collins, W.J., Barrata, V., Nordsvan, A.R., Pourteau, A., Li, Z.-X., Li, J., Beams, S., 2022. Spatio-temporal evolution of Mesoproterozoic magmatism in NE Australia: A hybrid tectonic model for Nuna assembly. Precambrian Res. 372. https://doi.org/10.1016/j.precamres.2022.106062.
Wan, B., Yang, X., Tian, X., Yuan, H., Kirscher, U., Mitchell, R.N., 2020. Seismological evidence for the earliest global subduction network at 2.0 Ga ago. Sci. Adv. 6. https://doi.org/10.1126/sciadv.abc5491.
Wang, C., Mitchell, R.M., Murphy, J.B., Peng, P., Spencer, C.J., 2021a. The role of megacontinents in the supercontinent cycle. Geology 49, 402–406.
Wang, P., Zhao, G., Liu, Q., Han, Y., Yao, J., Li, J., 2020. Zircons from Tarim basement provide insights into its positions in Columbia and Rodinia supercontinents. Precambr. Res. 341. https://doi.org/10.1016/j.precamres.2020.105621.
Wang, S., Sang, H., Qui, J., 1995. The forming ages of Yangzhuang and Wumishan Formations in Jixian section, Northern China. Sci. Geol. Sin. 30, 166–173.
Wang, W., Cawood, P.A., Pandit, M.K., 2021b. India in Nuna + Gondwana supercontinent cycles: Clues from the North Indian and Marwar block. Am. J. Sci. 321, 83–117.
Watson, G.S., 1956. Analysis of dispersion on a sphere. Monthly Notices of the Royal Astronomical Society. Geophysical Supplements 7, 153–159.
Weber, F., Gauthier-Lafaye, F., Whitechurch, H., Ulrich, M., El Albani, A., 2016. The 2-Ga Eburnian orogeny in Gabon and the opening of the Francevillian intracratonic basins. C.R. Geosci. https://doi.org/10.1016/j.crte.2016.07.003.
Williams, G.E., Schmidt, P.W., 2004. Neoproterozoic glaciation: reconciling low paleolatitudes and the geologic record. Geophys. Monogr. 146, 145–159.
Wingate, M.T.D., Pisarevsky, S.A., Gladkochub, D.P., Donskaya, T.V., Konstantinov, K.M., Mazubkabzov, A.M., Stanevich, A.M., 2009. Geochronologic and paleomagnetism of mafic igneous rocks in the Olenek Uplift, northern Siberia: implications for Mesoproterozoic supercontinents and paleogeography. Precambrian Res. 170, 256–266.
Whitmeyer, S.J., Karlstrom, K.E., 2007. Tectonic model for the Proterozoic growth of North America. Geosphere 3, 220–259.
Wu, G., Yang, S., Meert, J.G., Xiao, Y., Chen, Y., Wang, Z., Li, X., 2020. Two phases of Paleoproterozoic orogenesis in the Tarim craton: Implications for Columbia assembly. Gondwana Res. 83, 201–216.
Wu, H., Zhang, S., Li, Z.X., Li, H., Dong, J., 2005. New paleomagnetic results from the Yangzzhuang Formation of the Jixian System, North China and tectonic implications. Chin. Sci. Bull. 50, 1483–1489.
Xu, H., Yang, Z., Peng, P., Meert, J.G., Zhu, R., 2014. Paleoposition of the North China craton in the supercontinent Columbia: constraints from new paleomagnetic results. Precambrian Res. 255, 276–293.
Zhang, S., Li, Z.-X., Evans, D.A.D., Wu, H., Li, H., Dong, J., 2012. Pre-Rodinia supercontinent Nuna shaping up: A global synthesis with new paleomagnetic results from North China. Earth Planet Sci. Lett. 353–354, 145–155.
Zhang, S., Chang, L., Zhao, H., Ding, J., Xian, H., Li, H., Wu, H., Yang, T., 2021. Chapter 11. The Precambrian drift history and paleogeography of the Chinese cratons, in: Pesonen et al. (eds) Ancient Supercontinents and the Palaeogeography of the Earth, ISBN:978-0-12-818533-9, pp. 333-376.
Zhao, G., Cawood, P.A., Wilde, S.A., Sun, M., 2002. Review of global 2.1-1.8 Ga orogens: Implications for a pre-Rodinia supercontinent. Earth Sci. Rev. 59, 125–162.
Zhao, G., Sun, M., Wilde, S.A., 2003. Correlations between the eastern block of the North China craton and the South India Block of the Indian Shield: An Archean to Paleoproterozoic link. Precambrian Res. 122, 201–233.
Zhao, H., Li, S.Z., Sun, M., Wilde, S.A., 2004. A Paleo-Mesoproterozoic supercontinent: assembly, growth and breakup. Earth Sci Rev. 67, 91–123.
Zi, J-W., Sheppard, S., Muhling, J.R., Rasmussen, B., 2021. Refining the Paleoproterozoic tectonothermal history of the Penokean orogen: New U-Pb constraints from the Pembine-Wausau terrane, Wisconsin, USA. Bull, Geol. Soc. Am., doi:10.1130/B36114.1.

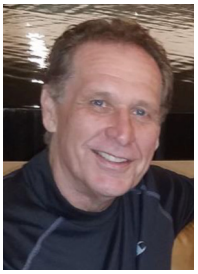

J.G. Meert is a professor in the Department of Earth and Planetary Sciences at the University of Florida in Gainesville, Florida (USA). Meert obtained his B.S. and M.S. degrees from the University of Florida in 1986 and 1988 respectively and completed his Ph.D. at the University of Michigan in 1993. He was involved in developing the first web presence for Gondwana Research in the 1990's and continues to serve as an Associate Editor of GR. Meert was President of IAGR from 2019-2022 and continues his service as Vice President. Meert is a fellow of the Geological Society of America and has published extensively on Precambrian paleomagnetism, geochronology and supercontinent history.

M. Santosh is a Professor at the CUGB, Specially Appointed Foreign Expert of China, Professor at the University of Adelaide, Australia and Emeritus Professor at the Faculty of Science, Kochi University, Japan. PhD (Cochin University of Science and Technology, India), D. Sc. (Osaka City University, Japan) and D.Sc. (University of Pretoria, South Africa). He is the Founding Editor of Gondwana Research as well as the founding Secretary General of the International Association for Gondwana Research. He is also the Editorial Advisor of Geoscience Frontiers and Geosystems and Geoenvironment. Research fields include petrology, fluid inclusions, geochemistry, geochronology, metallogeny, supercontinent tectonics and life evolution in the Early Earth. Published over 1300 research papers, edited several memoir volumes and journal special issues, and co-author of the book 'Continents and Supercontinents' (Oxford University Press, 2004). Recipient of National Mineral Award, Outstanding Geologist Award, Thomson Reuters 2012 Research Front Award, and Thomson Reuters/Clarivate High Cited Researcher Award during the last eight years.